

Worcester Polytechnic Institute Digital WPI

Masters Theses (All Theses, All Years)

Electronic Theses and Dissertations

2003-06-26

Removal of Hydrogen and Solid Particles from Molten Aluminum Alloys in the Rotating Impeller Degasser: Mathematical Models and Computer Simulations

Virendra S. Warke
Worcester Polytechnic Institute

Follow this and additional works at: <https://digitalcommons.wpi.edu/etd-theses>

Repository Citation

Warke, Virendra S., "Removal of Hydrogen and Solid Particles from Molten Aluminum Alloys in the Rotating Impeller Degasser: Mathematical Models and Computer Simulations" (2003). *Masters Theses (All Theses, All Years)*. 899.
<https://digitalcommons.wpi.edu/etd-theses/899>

This thesis is brought to you for free and open access by Digital WPI. It has been accepted for inclusion in Masters Theses (All Theses, All Years) by an authorized administrator of Digital WPI. For more information, please contact wpi-etd@wpi.edu.

**Removal of Hydrogen and Solid Particles from Molten
Aluminum Alloys in the Rotating Impeller Degasser:
Mathematical Models and Computer Simulations**

by

Virendra S. Warke

A thesis

Submitted to the faculty of the

WORCESTER POLYTECHNIC INSTITUTE

in partial fulfillment of the requirements for the degree of

Master of Science

in

Materials Science and Engineering

June 25, 2003

M.M. Makhoulf, Advisor

R.D. Sisson, Jr., Materials Science and Engineering Program Head

ABSTRACT

Aluminum alloy cleanliness has been in the limelight during the last three decades and still remains as one of the top concerns in the aluminum casting industry. In general, cleaning an aluminum alloy refers to minimizing the following contaminants: 1) dissolved gases, especially hydrogen, 2) alkaline elements, such as sodium, lithium, and calcium, and 3) unwanted solid particles, such as oxides, carbides, and a variety of intermetallic compounds. Extensive research has resulted in significant improvements in our understanding of the various aspects of these contaminants, and in many foundries, melt-cleansing practices have been established and are routinely used. However, with the ever-increasing demands for improved casting properties, requirements for molten metal cleanliness has become extremely stringent. Rotary degassing is one of the most efficient ways of cleansing molten metals, thus removal of unwanted particles and dissolved hydrogen from molten aluminum alloys by rotary degassing has become a widely used foundry practice. Rotary degassing involves purging a gas into the molten alloy through holes in a rotating impeller. Monatomic dissolved hydrogen either diffuses into these gas bubbles or it forms diatomic hydrogen gas at the bubbles' surface; in any case, it is removed from the melt with the rising bubbles. Simultaneously, solid particles in the melt collide with one another due to turbulence created by the impeller and form aggregates. These aggregates either settle to the furnace floor, or are captured by the rising gas bubbles and are also removed from the melt.

The objective of this work is to understand the physical mechanisms underlying the removal of dissolved hydrogen and unwanted solid particles from molten aluminum alloys by the rotating impeller degasser, and to develop a methodology for the effective

use of the degassing process by providing mathematical models and computer simulations of the process. The models and simulations can be used to optimize the process, design new equipment and determine the cause of specific operational problems.

ACKNOWLEDGMENTS

I am profoundly grateful to, Professor Makhlouf M. Makhlouf, Director of the Advance Casting Research Center, for being my advisor, for his energetic support and encouragement, and his valuable guidance and day to day advise throughout this research project. I would also like to express my appreciation to him for providing me the opportunity to carry out this research work.

I would like to offer special thanks to Professor Gretar Tryggvason, Head of the Mechanical Engineering Department, for his valuable guidance throughout the development of the computational fluid dynamics model in this research project. I would also like to thank Professor Diran Apelian, member of my advisory committee and Director of Metal Processing Institute, for offering encouraging discussions and valuable advise during the development of this work. Furthermore I am thankful to Professor Richard Sisson, Director of the Material Science and Engineering Program, for providing financial support through a teaching assistantship and also for being a member of my advisory committee.

I would also like to express my appreciation to Metal Processing Institute for the financial support during the summer. Special thanks are also due to Dr. Md. Maniruzzaman and Dr. Sumanth Shankar for their valuable help and time during this research project.

Finally I would like to thank my father, Sitaram, and mother, Sunita, for their understanding, patience, and inspiration provided by their love and tenderness.

Virendra Warke.

Table of Contents

	<u>Page</u>
Abstract	i
Acknowledgments	iii
Table of Contents	v
Chapter I: Introduction	1
Chapter II: Mathematical Modeling and Computer Simulation of Molten Metal Cleansing by the Rotating Impeller Degasser: Part I. Fluid Flow	6
Chapter III: Mathematical Modeling and Computer Simulation of Molten Aluminum Cleansing by the Rotating Impeller Degasser: Part II. Removal of Hydrogen Gas and Solid Particles	25
Appendix A: The CFD Simulation	55
Appendix B: The Particle Dynamics Simulation	63
Appendix C: The Hydrogen Removal Simulation	67

CHAPTER I

Introduction

Metal cleanliness is one of the major concerns in the Al casting industry due to the high demand for quality cast products. The presence of unwanted constituents above certain unacceptable level can have detrimental effects on the properties of the cast product, particularly its ductility, fatigue strength, fracture toughness, and machinability. These constituents could be dissolved gases such as hydrogen, solid particles such as oxides, carbides and intermetallic compounds, or alkaline elements such as Na, Li and Ca. There are various processes used to clean molten metal prior to casting. Filtration through cake filters or porous, rigid media filters, electromagnetic separation, and rotary degassing have been used successfully for the removal of solid particles. Similarly, natural degassing, vacuum degassing, and/or bubble degassing have been used for the removal of dissolved gases. This study is mainly focused on the rotary degassing (gas fluxing) as a process to remove both solid particles and dissolved hydrogen from molten aluminum alloys.

In the rotating impeller degassing process, a reactive or inert gas, or a combination of both types of gases is purged into the melt through a rotating impeller, or through a non-rotating immersed lance. The most commonly used inert gases are argon and nitrogen, and the most commonly used reactive gas is chlorine. Figure 1 shows a schematic of the process and illustrates the different mechanisms that occur during degassing.

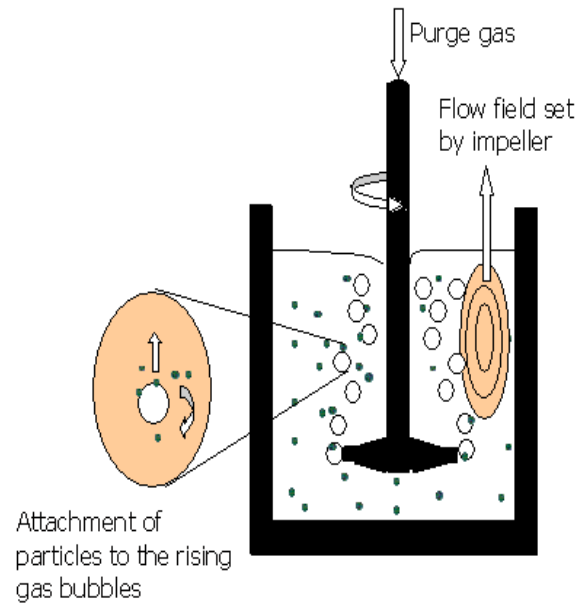


Fig. 1 – Schematic representation of rotary degassing process

The general mechanism of hydrogen removal is by diffusion of hydrogen across the metal/gas interface. Consequently, many factors influence hydrogen removal efficiency including alloy type, melt temperature, initial alloy hydrogen content, purge gas type and flow rate, purge gas/metal contact time, equipment efficiency, and external environmental conditions, such as the humidity of the surrounding air. If chlorine gas is used along with argon, a chemical reaction between dissolved hydrogen and Cl_2 occurs at the gas bubble surface, which enhances the efficiency of hydrogen removal from the melt. The addition of Cl_2 is also believed to change the surface tension at the gas/metal interface in such a way as to make trapping of the oxide particles at the bubble surface more efficient. In this work, the removal of hydrogen and solid particles from molten aluminum alloys by purging only argon gas through a rotating impeller is investigated

because it is the more commonly used method since HCl gas which is produced by the reaction of Cl₂ with hydrogen is environmentally hazardous.

The removal of solid particles from molten alloys in a rotating impeller flotation system involves two concurrent processes. Due to turbulence created by the rotating impeller, particles collide with one another and form clusters. These clusters form due to weak Van der Waal's forces of attraction between the solid particles. Once formed, the clusters either settle down to the bottom of the holding furnace due to the difference between their density and that of the melt, or they become captured by the rising gas bubbles and are taken away to the top surface of the melt, which is continuously skimmed off. These interactions depend largely on the flow field inside the melt, which is created by the impeller rotation and by the purge gas flow. The turbulence created by the impeller affects the particles' collision rate and hence the rate of formation of clusters which in turn affects the system's efficiency for removing solid particles.

RESEARCH OBJECTIVE

The main objective of this thesis is to characterize the mechanisms underlying the removal of dissolved hydrogen and unwanted solid particles from molten aluminum alloys in the rotating impeller degasser, and to develop a methodology for the efficient use of rotary degassers by providing mathematical models and computer simulations of the process.

In order to achieve this objective, a mathematical model is developed to simulate the rotating impeller degassing process for the removal of dissolved hydrogen and solid particles from molten aluminum alloys. The model is validated by comparing its predictions with experimentally obtained measurements. Computer simulations based on the model are then used to predict the effect of various process parameters on the process efficiency. In order to simplify the analysis and reduce the computation time, the rotary degassing process is divided into three different but interdependent processes each modeled by a dedicated module. These modules are (1) the Computational Fluid Dynamics (CFD) module, (2) The Particle Dynamics (PD) module, and (3) The Hydrogen Removal module. Figure 2 shows the interdependence of the three modules.

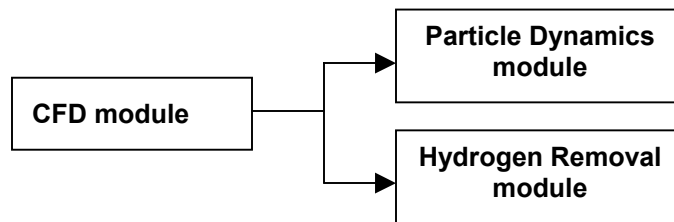


Fig. 2 – Simulation modules

THESIS ORGANISATION

The thesis is divided into three chapters: Chapter I is a brief introduction that provides an overview of the rotating impeller degassing process and states the objectives of the research program. Chapter II is an article that describes the Computational Fluid Dynamics module. The article is titled “*Mathematical Modeling and Computer Simulation of Molten Metal Cleansing by the Rotating Impeller Degasser: Part I. Fluid*

Flow”, and was submitted for publication in *Metallurgical and Materials Transactions*. Chapter III is an article that describes the Particle Dynamics and Hydrogen Removal modules. The article is titled “*Mathematical Modeling and Computer Simulation of Molten Metal Cleansing by the Rotating Impeller Degasser: Part II. Hydrogen and Particle Removal Model*”, and was also submitted for publication in *Metallurgical and Materials Transactions*.

CHAPTER II

Mathematical Modeling and Computer Simulation of Molten Metal Cleansing by the Rotating Impeller Degasser: Part I. Fluid Flow

V.S. Warke, G. Tryggvason, and M.M. Makhlof

The removal of dissolved hydrogen and solid impurity particles from molten alloys by rotary degassing is a widely used foundry practice. Rotary degassing involves purging a gas into the molten alloy through holes in a rotating impeller. Monatomic dissolved hydrogen either diffuses into these gas bubbles or it forms diatomic hydrogen gas at the bubbles' surface; in any case, hydrogen is removed from the melt with the rising bubbles. Simultaneously, solid particles in the melt collide with one another due to turbulence created by the impeller rotation and the gas flow and form aggregates. These aggregates either settle to the furnace floor, or are captured by the rising gas bubbles and are also removed from the melt. A mathematical model has been developed to simulate the turbulent multiphase flow field that develops in the melt during rotary degassing. The mathematical model allows calculation of the mean turbulence dissipation energy and the distribution of gas bubbles in the melt. Both these quantities are input into other mathematical models that simulate the removal of dissolved hydrogen and impurity solid particles from the melt.

I. INTRODUCTION

The presence of unwanted phases in molten alloys can cause a variety of property changes in cast components including an increase in porosity and modulus of elasticity, a reduction in fatigue strength and ductility, an increase in corrosion rate, and a reduction in electrical and thermal conductivity. In aluminum alloys, these unwanted phases are typically dissolved hydrogen, solid particles such as oxides, carbides and intermetallic compounds, and alkaline elements such as Na, Li and Ca. Consequently, the removal of these phases from molten alloys prior to casting is of vital importance to foundries. Rotary degassing is one of the most commonly used methods for removing dissolved hydrogen and unwanted solid particles from molten aluminum alloys. In a typical industrial degassing process, a gas, typically argon is purged through a rotating impeller into the liquid alloy. While the gas, in the form of discrete bubbles rises to the surface, monatomic dissolved hydrogen either diffuses into the bubbles or it forms diatomic hydrogen gas at the bubbles' surface; in any case, hydrogen is removed from the melt with the rising gas bubbles. Simultaneously, solid particles in the melt collide with one another due to the turbulence that is created by the impeller and the gas flow and form aggregates. These aggregates either settle to the furnace floor, or are captured by the rising gas bubbles and are also removed from the melt. Figure 1 is a schematic representation of a typical batch type rotary degassing unit. The efficiency of hydrogen removal from the melt depends to a large extent on the transfer coefficients of hydrogen at the melt/air and melt/bubble interfaces. Similarly, the efficiency of removal of solid particles from the melt depends largely on particle collisions with one another, particle

attachment to the gas bubbles, and the size and distribution of the gas bubbles. Ultimately, all these parameters depend on the flow field inside the melt.

Rotary degassing is very difficult to model since it encompasses a flow system that consists of multiple interacting phases, including a liquid phase (the molten alloy), two gaseous phases (the purged gas and dissolved hydrogen), and one or more solid phases (the unwanted solid particles). The difficulty in modeling such a system stems from the inability of current hardware to handle mathematical models that provide a detailed description of the flow field inside the melt including the turbulence created by the impeller rotation and gas flow, the interaction between the liquid and gas phases, the dynamics of the colliding solid particles, and the interaction between the purged gas and dissolved hydrogen. In order to simplify the analysis and make it amenable to solution, past efforts focused on the flow field induced by injected gas bubbles^[1,2,3]. For example, Johansen *et al.*^[4] and Hop *et al.*^[5] modeled the flow-field induced by the impeller by using single-phase transport equations. They assumed the purged gas, in the form of bubbles, is introduced into the computational domain as a dispersed phase and tracked its trajectory using a Lagrangian model. The removal efficiency of solid particles was computed based on the bubble trajectories along with the theory of particle deposition onto bubbles^[4,5]. Waz *et al.*^[6] used a similar approach and an Euler-Lagrangian model in order to model hydrogen removal from molten aluminum. In order to further simplify the model, Johanson *et al.*^[4], Hop *et al.*^[5] and Waz *et al.*^[6] restricted the motion of the melt's free surface and consequently excluded its effects on the flow field from their analysis. Recently, Maniruzzaman and Makhlof^[7] used an Euler-Euler multiphase approach to model the flow field in the rotary degasser. Maniruzzaman and Makhlof^[7],

^{8]} modeled the complex system that consists of multiple interacting phases as two separate but interdependent subsystems. The first subsystem deals with the turbulent flow field arising from the impeller rotation and gas flow, and the second subsystem deals with the particle dynamics. By modeling the two subsystems separately, it was possible to include more complexity into the models without taxing computer time. Particularly, the Maniruzzaman and Makhlof computational fluid dynamics model allows movement of the melt's free surface and thus their model can reflect possible *vortexing* at the melt's surface. However, in their CFD model, Maniruzzaman and Makhlof ^[7] used 2-dimensional axi-symmetric geometry in order to minimize computing time. Moreover, their overall model did not address the removal of dissolved hydrogen from the melt. Nevertheless, in this work, we adopt the approach originally devised by Maniruzzaman and Makhlof ^[7] and model the rotating impeller degasser as composed of three separate but inter-related subsystems. The first subsystem, which is the subject of this article, deals with the turbulent flow field arising from the impeller rotation and gas flow. Standard fluid flow and turbulence equations are used in modeling this subsystem, and the complex multiphase fluid flow is formulated using an Eulerian discrete phase model. A special computational fluid dynamics (CFD) code that is based on an Euler-Euler approach ^[9,10] is employed in the computer simulation. The second subsystem deals with the particle dynamics, and its model, which is heavily based on the recent work by Maniruzzaman and Makhlof ^[8], accepts input from the flow field simulation in the form of turbulence dissipation energy and bubble distribution. The third subsystem deals with the removal of dissolved hydrogen, and, similar to the particle dynamics subsystem, its model accepts input from the flow field simulation in the form bubble

distribution. The particle dynamics model and the model for removal of dissolved hydrogen are the subject of Part II of this two-part article.

II. THE MATHEMATICAL MODEL

Flow inside the melt is fully turbulent and multiphasic ^[4,5,7]. In this model, the two phases – molten metal and purge gas – are treated separate from one another by solving two sets of momentum and continuity equations. Subsequent coupling of the solutions is achieved through pressure and inter-phase exchange coefficients ^[10]. In order to model complex impeller shapes, 3-dimensional modeling with multiple reference frames is used ^[10]. The Eulerian multiphase ^[9,10] method and a κ - ε model with standard formulation for turbulence calculations are used to fully model the fluid flow. The fluid is divided into two zones ^[10]: a cylindrical zone around the impeller blades, which is separated from the rest of the melt by grid interfaces, and the rest of the melt. The inner cylindrical zone around the impeller is modeled using a rotating reference frame whose rotation velocity is taken as the impeller speed while the velocity of the impeller is set to zero relative to this reference frame. The rest of the fluid is treated as a stationary reference frame. All fluid properties are shared between the two zones at the grid interfaces. In the Eulerian multiphase method, the different phases are treated mathematically as interpenetrating continua and the volume fractions of all phases are assumed to be continuous in space and time, and their sum is equal to one. Among the various methods available for modeling multiphasic flow, the Euler method is the most suitable for modeling very fine dispersed phases and is preferred over the Volume of Fluid (VOF) method, which is typically useful for free surface calculations and for modeling homogeneous multiphase

flows^[10]. Two sets of momentum and continuity equations are solved; one set for each of the two phases and coupling is achieved through pressure and inter-phase exchange coefficients. Many models with varying complexity have been used to represent turbulent flow. These models range from the simple mixing length model^[13] to the more complex large eddy models^[12,13]. The κ - ε model is a reasonable compromise between the two extremes. The standard κ - ε model is a semi empirical model based on transport equations for the turbulence kinetic energy (κ) and its dissipation rate (ε). The transport equation for κ is obtained from the exact equations, while the transport equation for ε is obtained using physical reasoning^[10,11]. The two transport equations are solved throughout the domain in order to obtain κ and ε . The κ - ε model assumes that flow is fully turbulent, and that the effects of molecular viscosities are negligible^[11]. Moreover, in the κ - ε model, the Reynolds stresses are assumed proportional to the mean velocity gradient where the constant of proportionality is viscosity^[13].

Although it is possible in this model to allow movement of the melt's free surface, movement of the melt's free surface was restricted since allowing the free surface to move requires the introduction of an additional phase, namely air, at the free surface, which will substantially tax computer time.

III. SOLUTION PROCEDURE AND BOUNDARY CONDITIONS

The fluid flow pattern, the gas bubble distribution, the turbulent energy dissipation rate, and the pressure contours in the melt are determined by solving the model presented in the section II. Figure 2 shows a flow diagram representing the solution procedure. First,

a 3-dimensional representation of the geometry is created. A mesh, consisting of 84,442 tetrahedral cells is then generated throughout the domain using a finer mesh size to represent the fluid zone between the impeller blades and the grid interface than the mesh size used for the bulk of the fluid. The mesh is imported into the commercial software FLUENT 6.0.2 solver and the solution is obtained in two stages.

FLUENT V6.0.2 is marketed by Fluent, Inc. (Lebanon, NH).

First, the steady-state solution is obtained for a single-phase flow field, i.e., a flow field with no gas purging. A moving reference frame that rotates with the desired angular velocity is used to model the boundary between the fluid zone surrounding the impeller and the grid interface. A similar boundary condition is imposed on the impeller's shaft. On the other hand, a wall rotating with zero angular momentum relative to the rotating reference frame is used to model the boundary condition at the impeller's surface and the gas outlets. The top surface of the tank is set as a pressure outlet, and the tank walls are modeled as stationary walls. All other surfaces are assumed to be no-slip walls where the shear stresses are approximated by a semi-empirical wall function^[10]. Once the steady-state solution is obtained, it is used as an initial guess for the transient solution. It is important to note that while in its standard format the multiple reference frame procedure can be used for steady state calculations, special modifications are necessary for its use in transient conditions^[10]. All the boundary conditions used to obtain the steady-state solution are retained in the multi-phase transient solution, except for the boundary condition used to model the gas outlets into the melt. The boundary condition at the gas outlets into the melt is set to a pre-calculated velocity magnitude and the volume fraction of gas at the outlet is set to one. The gas velocity is calculated by assuming that the gas

behaves ideally and applying the necessary pressure and temperature corrections. In order to determine the gas temperature at the gas outlets, a heat transfer mathematical model of the impeller is constructed. The mathematical model is solved using the heat transfer module in FLUENT 6.0.2. In order to simplify the analysis, a 2-D model of the impeller is used and the outer walls of the impeller are set to a constant temperature, which is the temperature of the molten metal. Figure 3 shows the temperature distribution in the impeller and the gas flowing within it. The velocity at the gas outlets is computed by constructing a mass balance on the flow of the gas. The volume fraction of each phase and the turbulent energy dissipation rate are calculated using volume averaged fluid properties.

IV. APPLICATION OF THE MATHEMATICAL MODEL

The mathematical model presented in the preceding sections is used to calculate the fluid flow in a holding furnace during rotary degassing. A cylindrical crucible and a laboratory scale degasser with the impeller represented schematically in Figure 4 were used in the simulation. The dimensions of the crucible and impeller are presented in Table I, and the relevant properties of the molten aluminum alloy and argon purge gas are presented in Table II. Figure 5 shows the simulated change of volume fraction of purge gas in the melt with purging time and shows that a constant process is established after about 16 seconds of rotary degassing. Therefore, simulating only the first 24 seconds of the process is sufficient to determine the energy dissipation rate and the volume fraction of gas in the melt.

Figure 6 shows the simulated velocity vectors inside the molten alloy with the impeller rotating at 600 rpm and a gas flow rate of 5 lit/min. The figure shows the typical recirculation patterns that are expected in stirred melts. Also, as expected, the magnitudes of the velocity vectors at the impeller are high compared to their counterparts at the crucible's wall. Similarly, Figure 7 shows the distribution of purge gas inside the molten alloy with the impeller rotating at 600 rpm and a gas flow rate of 5 lit/min.

Table I. Dimensions of the Crucible and Impeller used in the Computer Simulations.

Parameter	Dimension
Crucible diameter	21.5 cm
Crucible height	35.5 cm
Melt depth	23 cm
Impeller shaft diameter	3.8 cm
Impeller disk diameter	10.2 cm
Number of gas outlets	4
Diameter of the gas outlets	1.5 mm
Impeller height from the bottom of the crucible	7.5 cm

Table II. Physical Properties of Molten Aluminum Alloy and Argon Gas.

Molten Aluminum at 973 K

Density	2300 kg/m ³
Viscosity	0.0029 Pa-s
Surface tension	0.9 N/m
Kinematic viscosity	1.3 × 10 ⁻⁶ m ² /s

Argon gas at 298 K

Density	1.6228 kg/m ³
Viscosity	2.125 × 10 ⁻⁵ Pa-s

Note that, under these process conditions, the distribution of purge gas inside the melt is localized around the impeller shaft. This is caused by the pressure distribution in the melt that creates a relatively low-pressure zone around the impeller shaft and presents, at this location, relatively low resistance to the escaping gas. Figure 8 shows vertical pressure

contours inside the melt, and Figure 9 shows the radial variation of the volume fraction of purge gas and the radial variation of pressure on a horizontal plane within the melt. These pressure profiles are characteristic to the geometry of the system that is simulated and reflect a non-ideal ratio of rotor disc diameter to crucible diameter. The relatively large diameter of the disc compared to the diameter of the crucible creates the observed pressure profile, which confines the bubbles to a relatively narrow volume surrounding the impeller shaft.

V. SUMMARY

A mathematical model for simulating the flow field inside molten alloys during rotary degassing is developed. The multiple reference frame method is used to obtain the transient solution to the complex multiphase fluid flow problem. The model gives much needed insight into the mechanics of melt flow during rotary degassing and may be used to simulate batch type flotation melt treatment processes. In this case, the model results, in the form of mean values of purge gas volume fraction and energy dissipation rate are input into the mathematical models presented in Part II of this two-part paper in order to simulate the removal of unwanted solid particles and dissolved hydrogen from molten alloys.

ACKNOWLEDGMENT

The authors gratefully acknowledge Dr. Md. Maniruzzaman for his assistance and stimulating discussions throughout this project.

REFERENCES

1. S. T. Johansen and F. Boysan: Metall. Trans. B, 1986, vol. 19B, pp. 755-764.
2. O. J. Ilegbusi and J. Szekely: ISIJ Int., 1990, vol. 30, pp. 731-739.
3. O. J. Ilegbusi and J. Szekely: International Symposium on Injection in Process Metallurgy, 1991, pp. 1-34.
4. S. T. Johansen, A. Fredriksen, and B. Rasch: Light Met., 1995, pp. 1203-1206.
5. B. I. Hop, S. T. Johansen, and B. Rasch: EPD Congress, 1996, pp. 647-656.
6. E. Waz et al, Light metals 2003, TMS 132nd International conference, 2003, pp. 901-907.
7. M. Maniruzzaman and M. Makhlof, Metall. Trans, B, 2001, pp.297-303.
8. M. Maniruzzaman and M. Makhlof, Metall. Trans, B, 2001, pp.305-313.
9. C. Crowe, M. Sommerfeld, and Y. Tsuji: Multiphase Flows with Droplets and Particles, CRC Press, Boca Raton, 1997.
10. FLUENT: FLUENT User's Guide, FLUENT Inc., Lebanon, New Hampshire, 1996, vol. 1-5.
11. B.E. Launder and D. B. Spalding: Lectures in Mathematical Models of Turbulence, Academic Press, London, 1972.
12. O. J. Ilegbusi, M. Iguchi, and W. Wahnsiedler: Mathematical and Physical Modeling of Materials Processing Operations, Chapman & Hall/CRC, Boca Raton, 1999.
13. J. Derksen and H.E.A.V.d. Akker: *AIChE J.*, 1999, vol.45, pp.209-21.

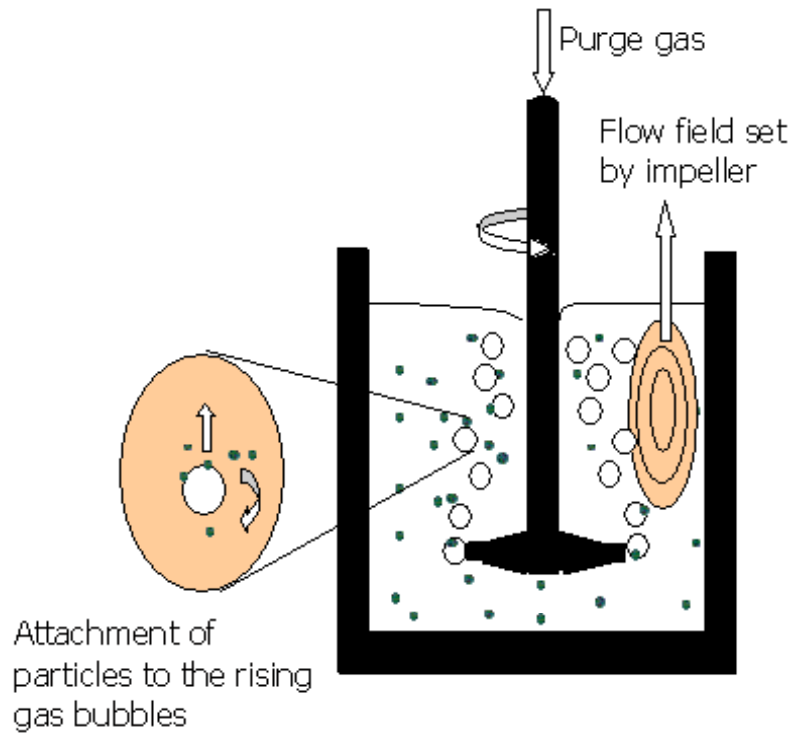


Fig. 1 – Schematic representation of the rotary degassing process.

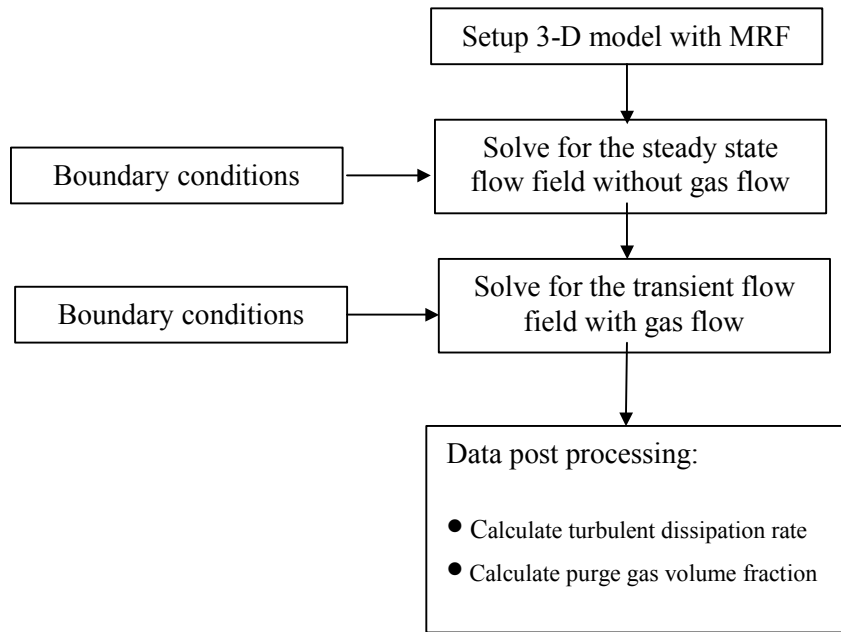
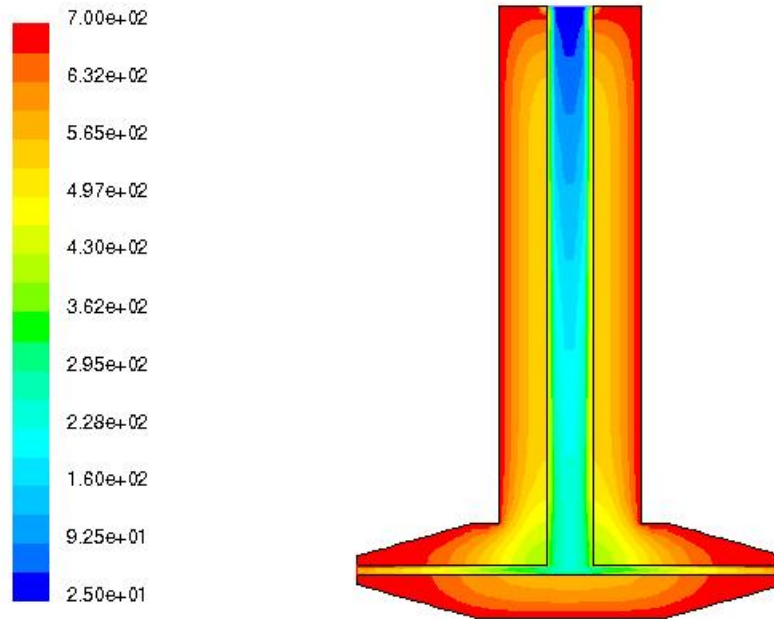
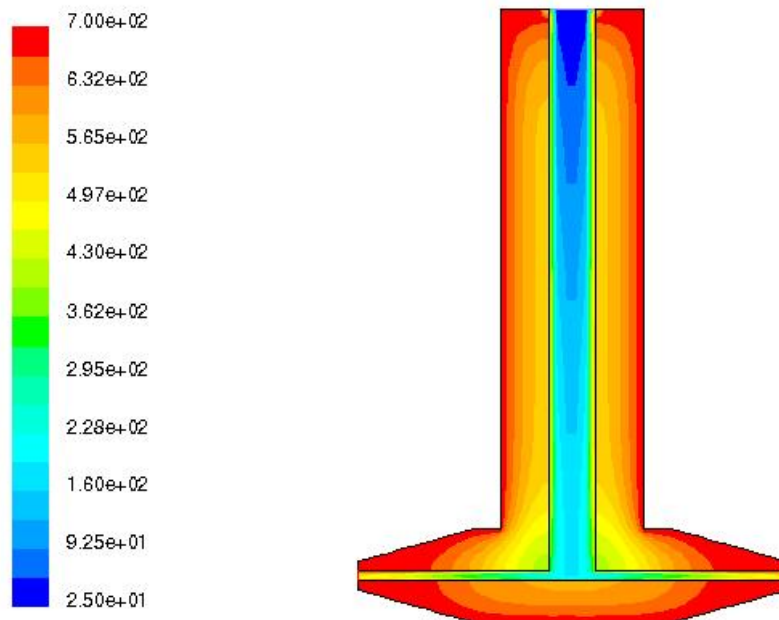


Fig. 2 – Flow chart describing the solution procedure.



(a)



(b)

Figure-3: Temperature distribution in argon gas flowing through the graphite impeller
(a) gas flow rate = 3 L/min and (b) gas flow rate = 5 L/min

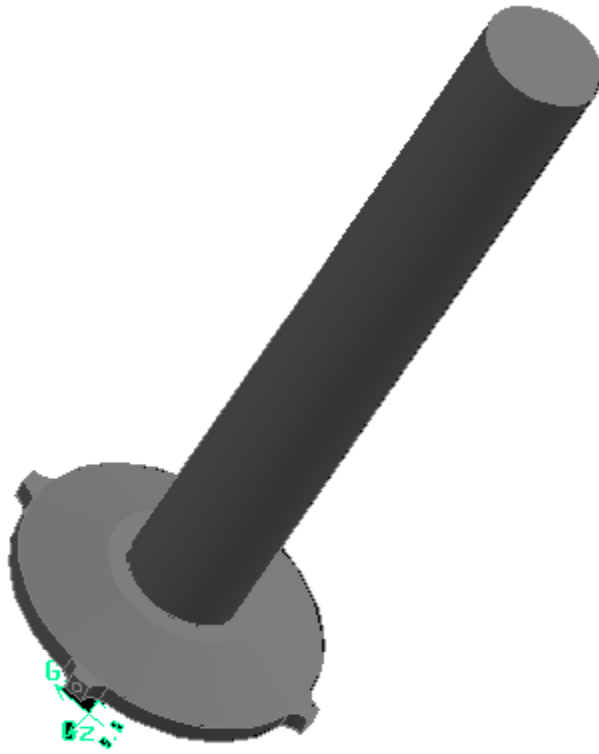


Figure-4: Schematic representation of the impeller.

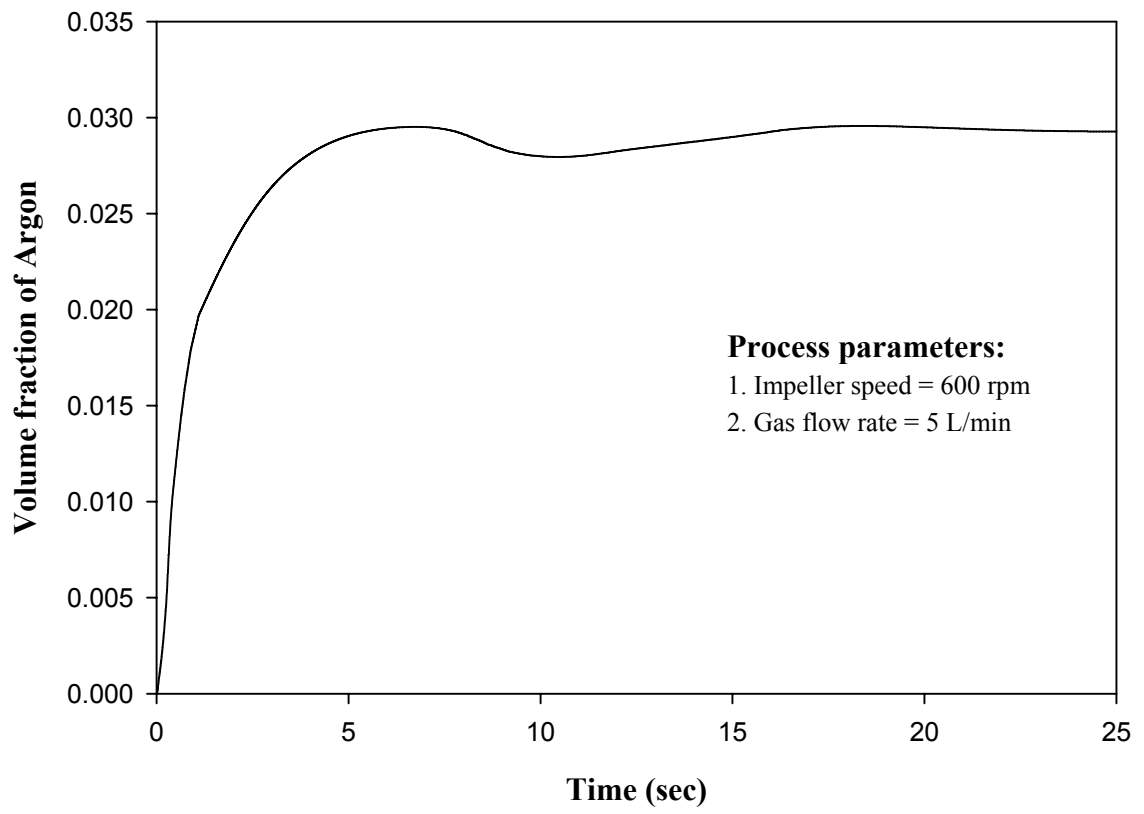


Figure-5: Variation of the volume fraction of purge gas with purging time. The impeller speed is 600 rpm and the gas flow rate is 5 lit/min.

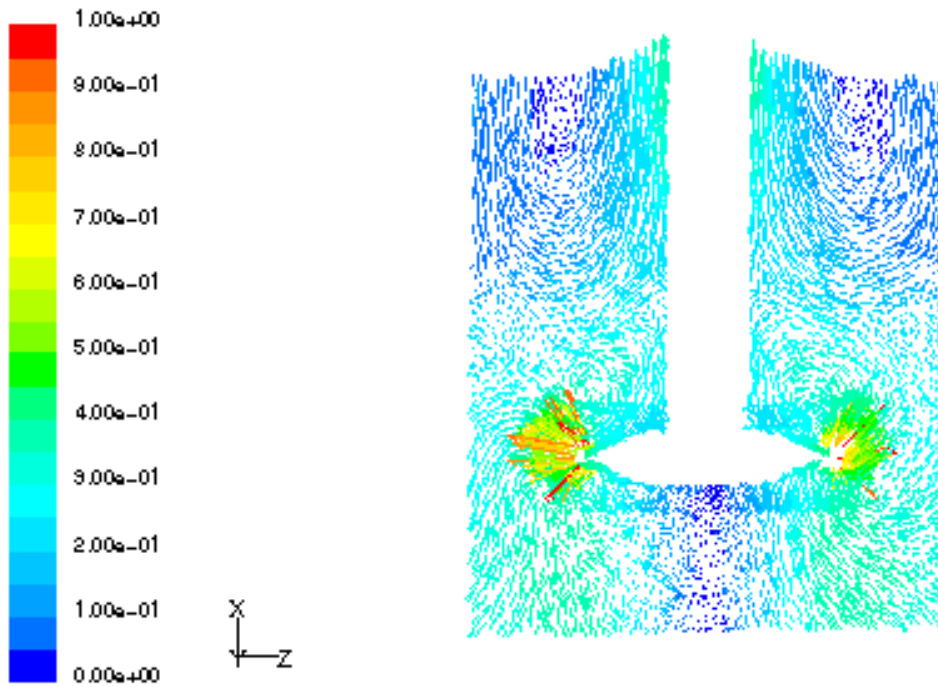


Figure-6: Simulated velocity vectors on an X-Z plane within the melt after 24 seconds of gas purging. The impeller speed is 600 rpm and the gas flow rate is 5 lit/min.

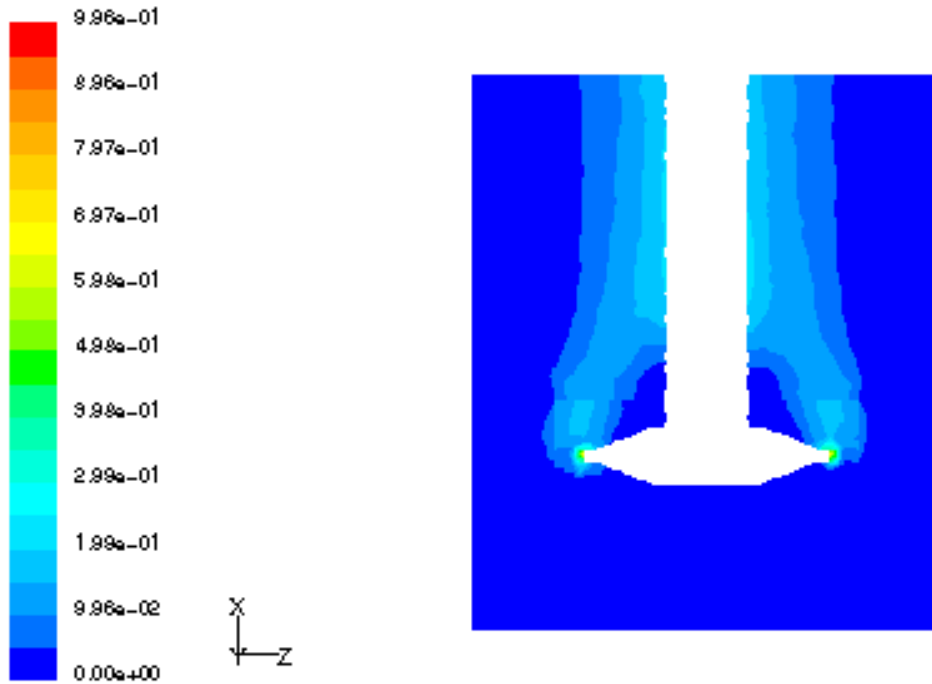


Figure-7: Simulated contours of volume fraction purge gas on an X-Z plane within the melt after 24 seconds of gas purging. The impeller speed is 600 rpm and the gas flow rate is 5 lit/min.

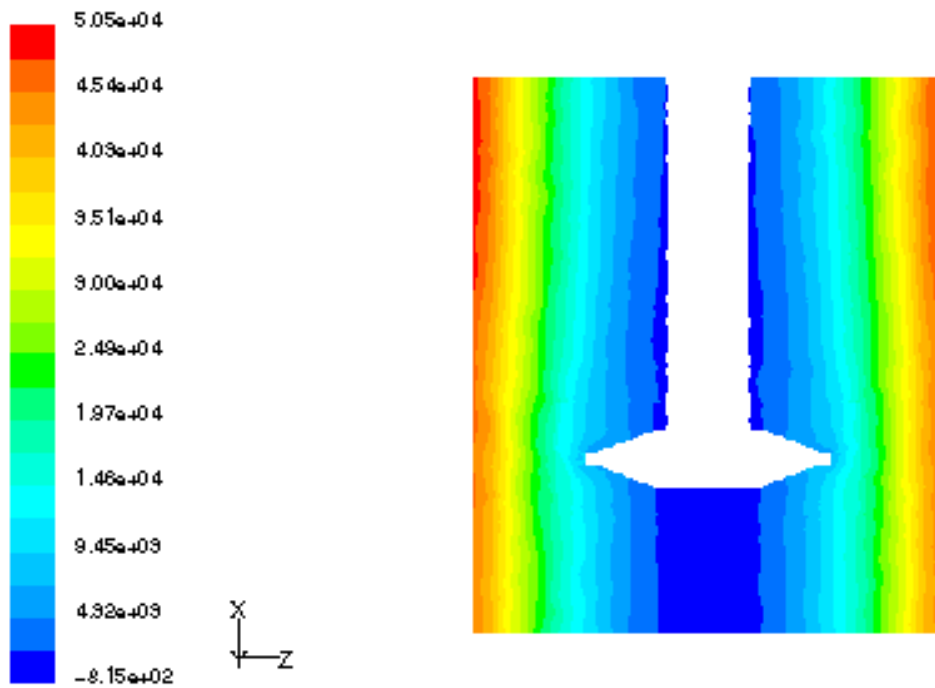
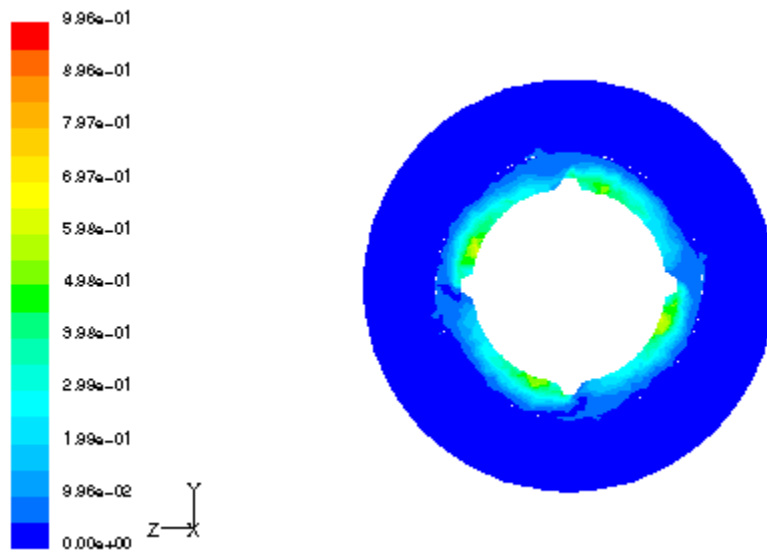
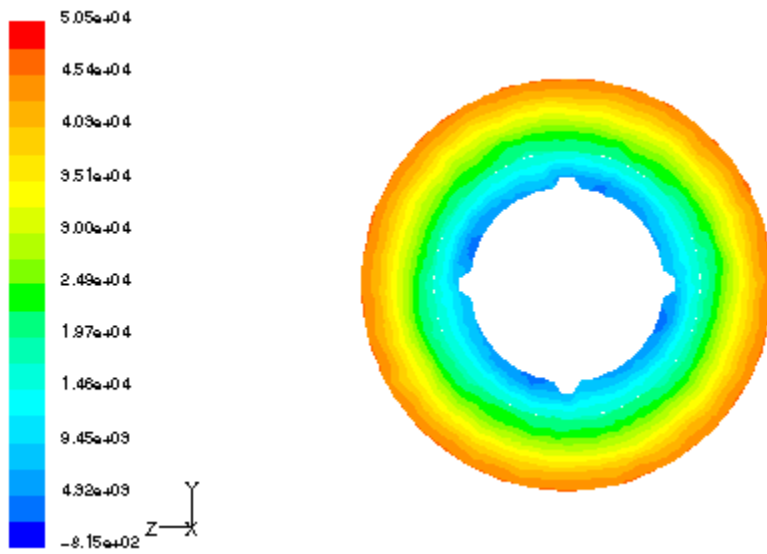


Figure-8: Simulated contours of pressure on an X-Z plane within the melt after 24 seconds of gas purging. The impeller speed is 600 rpm and the gas flow rate is 5 lit/min.



(a)



(b)

Figure-9: Simulated contours on an Y-Z plane of (a) volume fraction of purge gas, and (b) pressure after 24 seconds of purging. The impeller speed is 600 rpm and the gas flow rate is 5 lit/min.

Chapter III

Mathematical Modeling and Computer Simulation of Molten Aluminum Cleansing by the Rotating Impeller Degasser: Part II. Removal of Hydrogen Gas and Solid Particles

V.S. Warke, S. Shankar, and M.M. Makhlouf

Rotary degassing is widely used in the foundry industry for removing hydrogen gas and solid impurities from molten aluminum alloys. In this method, a specially designed impeller rotates inside the melt and gas is purged into the molten alloy through holes located at the bottom of the impeller. The purged gas forms bubbles that rise to the melt's surface. While rising, the bubbles pick up hydrogen gas and solid impurities from the melt and carry them to the surface where they are incorporated into the sludge layer. Removal of hydrogen from the melt is essentially a consequence of diffusion of the dissolved hydrogen from the melt into the rising gas bubbles, and removal of solid particles is a consequence of their clustering and settling, as well as their attachment to the rising gas bubbles. A mathematical model is developed to simulate the removal of hydrogen and unwanted solid particles from aluminum alloy melts. Hydrogen removal is modeled by applying conservation of mass to the melt and developing a hydrogen mass balance. Similarly, particle removal is modeled by applying a special particle population balance. This model is comprehensive as it allows simulation of the entire rotary degassing melt-cleansing process including the removal of unwanted particles and hydrogen gas.

I. INTRODUCTION

Aluminum alloys are susceptible to degradation during melting and melt holding even when optimum conditions are used. The detrimental effects of time at temperature on the quality of molten aluminum alloys are well documented ^[1] and include adsorption of hydrogen gas, and melt oxidation and contamination. Hydrogen is the only gas that is appreciably soluble in aluminum, and its solubility varies directly with temperature. The solubility of hydrogen in aluminum just above and just below the melting point is 0.65 and 0.034 mL/100g, respectively ^[2], and these values vary only slightly with alloy content. Consequently, during the solidification of molten aluminum alloys, dissolved hydrogen in excess of the maximum solid solubility precipitates out in molecular form and forms what is known as hydrogen porosity. Aluminum and its alloys oxidize readily by direct oxidation in air and by reaction with water vapor. Melt oxidation results not only in costly melt losses and unwanted alteration in alloy chemistry, but also in the formation of brittle complex oxide particles that may be entrained into the melt's bulk ^[3]. In addition to oxides, a number of other compounds can be present in molten aluminum, including aluminum carbide that forms during reduction, and borides that can agglomerate and represent a significant factor in the metal structure ^[3]. Hydrogen porosity and entrained particles strongly influence the mechanical properties of aluminum alloy castings ^[2]. Consequently, various melt treatment techniques have been developed and are employed to minimize the hydrogen concentration and the incidence of unwanted particles in molten aluminum alloys ^[2,3]. Rotary degassing, which is represented schematically in Figure 1, is one of the most widely used techniques for removing hydrogen and unwanted particles from molten aluminum. In this process, an inert gas, or

a mixture of a reactive and an inert gas is injected through the shaft of a rotating impeller and is released through fine openings at the base of the rotor into the liquid alloy.

The most commonly used inert gases are argon and nitrogen and the most commonly used reactive gases are chlorine and fluorine. Reactive gases are used in low concentration of under 10%. Even in these low concentrations, both chlorine and fluorine have significant effects on bubble surface tension and in wetting out inclusions from the melt ^[4-7].

The high speed rotation of the impeller shears the gas bubbles as they are released and produces a very fine and widely dispersed bubble pattern within the melt. The purge gas bubbles collect hydrogen from the melt because of the lower partial pressure of hydrogen presented by the purge gas bubble in comparison to the surrounding melt. Hydrogen diffuses into the purge gas bubbles, which rise to the surface of the melt and are expelled into the atmosphere. Therefore, the efficiency of hydrogen removal by the rotary degasser depends on several interrelated factors including the initial hydrogen content of the melt, the holding vessel size, the purge gas flow rate (which, in conjunction with the vessel size, determines the bubbles' residence time in the melt), the mixing capability of the rotor, and alloy specific thermodynamic factors and mass transfer coefficients. The purge gas bubbles collect the unwanted particles from the melt by de-wetting the oxide/metal interface to provide enhanced separation of the solid particles from the melt (when a reactive gas is used) and flotation of the particles by attachment to the rising gas bubbles. The turbulent field inside the melt increases the probability of capture of the particles by the gas bubbles and causes collisions and clustering of the particles, which enhances their settling to the holding vessel's floor. Therefore, the efficiency of particle removal by the rotary degasser depends on the flow field inside the melt created by the impeller rotation and gas flow. The velocity and turbulence fields in the melt govern the transport of particles to the bubbles' surfaces, and the addition of reactive gases to the

purge gas affects the surface tension of the bubbles in such a way as to enhance separation of the solid particles from the melt.

Historically, the optimization of rotary degassers and degassing processes relied to a large extent on operator experience, but better understanding and more effective use of the process may be achieved through mathematical modeling and computer simulations. An effective way of mathematically describing the removal of hydrogen from molten aluminum in a rotary degasser is by means of a hydrogen mass balance. Conservation of hydrogen is applied globally to the melt assuming that the melt is well mixed so that the hydrogen concentration within it does not change with spatial co-ordinates. Similarly, an effective way of mathematically describing removal of solid particles from molten aluminum in a rotary degasser is by means of a particle population balance that describes particle clustering, sedimentation, and flotation. In this publication, mathematical models are presented to describe (i) the transport of hydrogen from the bulk of molten aluminum to the purge gas bubbles and its subsequent removal from the melt by the rising purge gas bubbles, and (ii) the dynamics of particle clustering, and particle removal from the melt by sedimentation to the holding vessel's floor and by flotation to the surface layer with the rising purge gas bubbles. While this presentation is limited to batch type rotary degassers, it may easily be extended to include in-line systems. The models are used to investigate the effect of the rotary degasser's operational parameters on the removal of hydrogen and solid particles from molten aluminum and are useful in designing efficient rotary degassing systems and in selecting the operation parameters for optimum degasser performance.

II. THE MATHEMATICAL MODELS

A. The Hydrogen Removal Model

Although there are many potential sources for hydrogen in aluminum alloys, including crucible walls, charge materials, fluxes, and furnace tools, the main source of hydrogen in aluminum alloys is water vapor from the atmosphere surrounding the melting and holding furnaces. Water vapor from the atmosphere diffuses into the melt's surface where it reacts with molten aluminum according to Eq. [1]



A fraction of the hydrogen produced by this reaction exits the melt's surface to the atmosphere, and the rest diffuses into the melt's bulk in the form of monatomic hydrogen [1,8]. The instantaneous concentration of hydrogen in the melt may be described by the general mass balance equation, which is obtained by applying conservation of hydrogen to the melt, and assuming that the melt is well mixed so that the hydrogen concentration within it does not change with spatial co-ordinates.

$$[K_s \cdot A_s \cdot (C^{eq} - C)] - [K_b \cdot A_b \cdot (C - C^b)] = V_{Al} \cdot \frac{dC}{dt} \quad [2]$$

The first term in Eq. [2] represents the flux of hydrogen entering the melt from the atmosphere, the second term represents the flux of hydrogen exiting the melt to the atmosphere, and the term on the right of Eq. [2] represents the rate of change of hydrogen concentration within the melt. If the concentration of hydrogen at the center of the bubble, C^b , is assumed zero, then Eq. [2] reduces to Eq. [3]

$$[K_s \cdot A_s \cdot (C^{eq} - C)] - [K_b \cdot A_b \cdot C] = V_{Al} \cdot \frac{dC}{dt} \quad [3]$$

The total surface area of bubbles is calculated from computational fluid dynamics simulation of the rotary degasser ^[9], and the average stable bubble radius is calculated using Hinze's formula ^[10] modified for a rotary degasser ^[11,12],

$$r_b = \frac{1}{2} D \left(\frac{Q_g}{Q_{go}} \right)^m \left(\frac{We_c \sigma}{\rho} \right)^{0.6} \frac{1}{\varepsilon^{0.4}} \quad [4]$$

In Eq. [4], $Q_{go} = 25$ l/min, $D = 0.878$, $m = 0.28$, and Q_g is the gas flow rate in l/min, and a critical Webber number, $We_c \approx 4$, is necessary for the bubble to be stable ^[13].

The Al_2O_3 that forms in reaction [1] is essentially protective since its Pilling Bedworth ratio is greater than one ^[14], and, in addition to preventing further oxidation of the melt; it reduces the rate of hydrogen entry into the melt's surface. As a result, the concentration of hydrogen in the melt's surface quickly reaches an essentially constant equilibrium value that is dictated by the humidity of the atmosphere surrounding the furnace, C^{eq} . Bakke et al proposed a theoretical relation to calculate the equilibrium hydrogen concentration at the melt/atmosphere interface of a stagnant aluminum melt [8]. However, the Bakke et al equation cannot be used to calculate the concentration of hydrogen at the melt/atmosphere interface during rotary degassing since the impeller rotation significantly affects the kinetics of the reaction in Eq. [1]. Alternately, this necessary boundary condition, together with the mass transfer coefficient at the melt/air interface, K_s and the mass transfer coefficient at the melt/bubble interface, K_b , are obtained using a semi-empirical approach.

Determination of the model constants – C^{eq} , K_s , and K_b

Commercial purity aluminum is held at $700\pm 5^\circ\text{C}$ in a cylindrical crucible. The dimensions of the crucible and impeller are shown in Table I. A laboratory size rotary degasser is used to stir the melt without passage of argon gas, and the concentration of hydrogen in the melt is measured at specific time intervals using a hydrogen analyzer and the data is plotted in Figure 2.

AlScan™ manufactured by ABB Bomem Inc., Quebec, Canada.

Table I. Dimensions of the Crucible and Impeller.

Crucible diameter	21.5 cm
Crucible height	35.5 cm
Melt depth	23 cm
Impeller shaft diameter	3.8 cm
Impeller disk diameter	10.2 cm
Number of gas outlets	4
Diameter of gas outlet	1.5 mm
Impeller elevation from furnace floor	7.5 cm

Since no gas is purged into the melt, Eq. [3], which represents the overall hydrogen balance, reduces to Eq. [5], which describes the change in hydrogen concentration in the melt due only to hydrogen uptake from the atmosphere,

$$K_s \cdot A_s \cdot (C^{eq} - C) = V_{Al} \cdot \frac{dC}{dt} \quad (5)$$

The solution to Eq. [5] is Eq. [6]

$$C = C^{eq} - \left((C^{eq} - C_o) \cdot \exp\left(\frac{-K_s \cdot A_s}{V_{Al}} \cdot t \right) \right) \quad (6)$$

The curve representing Eq. [6] is fitted to the data points in Figure 2 using regression analysis, and the parameters K_s and C^{eq} are thus obtained. Similar experiments are performed using different impeller rotation speeds and in each case the values of K_s and C^{eq} are obtained. Table II and Figure 3 show the variation of K_s with rotation speed.

Table II. Experimentally Obtained Values for the Overall Mass Transfer Coefficient at Melt/Air Interface (K_s) and the Concentration of Hydrogen at the Melt/Air Interface (C^{eq}).

Impeller speed (rpm)	Dew point temperature (°F)	C^{eq} (ml/100g)	K_s ($\times 10^3$ cm/s)
150	28	0.2200	7.52
300	28	0.2667	10.03
450	23	0.2335	12.30
600	10	0.2919	21.40

In order to determine K_b , similar measurements are performed on the melt, but in this case a 99% purity argon gas is purged through the rotating impeller into the melt and Eq. [3] is solved to give

$$C = \left(\frac{K_1 \cdot C^{eq}}{(K_1 + K_2)} \right) - \left(\frac{K_1 \cdot C^{eq} - (K_1 + K_2) \cdot C_o}{(K_1 + K_2)} \exp\left(\frac{-(K_1 + K_2)}{V_{Al}} \cdot t \right) \right) \quad [7]$$

where $K_1 = K_s A_s$ and $K_2 = K_b A_b$. Values for K_s and C^{eq} are obtained from Table III, and A_b is obtained by calculating the average stable bubble radius using Eq. [3] and the volume fraction of gas in the melt. Table III shows the change in K_b with impeller rotation speed. Note that K_b remains essentially constant with impeller rotation speed and with gas flow rate.

Table III. Total Surface Area of Bubbles (A_b) and Overall Mass Transfer Coefficient of Hydrogen at the Melt/Gas Interface (K_b).

Impeller Speed (rpm)	Gas Flow Rate (L/min)	A_b (cm ²) [♦]	K_b (cm/s)
150	3	94.181	0.0761
300	3	170.596	0.0799
450	3	197.143	0.0783
600	5	444.25	0.0797

[♦]Obtained from CDF simulations [9].

B. The Particle Dynamics Model

Solid particles suspended in molten metal and continuously interacting with each other, aggregating and being removed from the domain by attaching to rising gas bubbles, or settling to the furnace floor is best described mathematically using a particles population balance equation such as that given in Eq. [8]^[15]. The solution to the particles population balance equation gives the change in the particle size distribution density with time and allows tracking the removal of particles from the melt.

$$\begin{aligned} \frac{\partial n_v(v, t)}{\partial t} = & -\frac{\partial}{\partial v} [I_v(v, t) n_v(v, t)] + \int_0^{v/2} W_v(v - \tilde{v}, \tilde{v}) n_v(v - \tilde{v}, t) n_v(\tilde{v}, t) d\tilde{v} \\ & - n_v(v, t) \int_0^\infty W_v(v, \tilde{v}) n_v(\tilde{v}, t) d\tilde{v} + S_v[n_v(v, t), v, t] \end{aligned} \quad [8]$$

Eq. [8] describes the particle size distribution density function, $n_v(v, t)$, where $n_v(v, t) dv$ is the number of particles with a volume in the range v to $(v+dv)$ per unit volume of fluid. Although the mathematical formulation of the population balance equation is simple, it can only be solved analytically for specialized cases. Consequently, many approximation techniques were developed for solving the population balance equation^[16,17,18]. These include (a) describing the particle size distribution using a continuous function, which was shown to be an accurate procedure but requires excessive time, (b) approximating the

particle size distribution using a parameterized lognormal function, which is relatively fast but has limited accuracy, (c) describing the particle size distribution function by its moments, which is less accurate than the preceding two methods because it yields only the average properties over the range of particle size distribution, and (d) discretizing the population balance equation, where the continuous particle size distribution is approximated by a finite number of sections with the properties within each section averaged. This method is accurate, but it usually requires a large number of sections in order to produce a satisfactory solution; therefore it is computer time intensive ^[16,17]. In order to overcome this difficulty, the continuous population balance equation is replaced with a set of discretized equations with particle volume as an internal co-ordinate ^[13,19]. Hence, the discretized population balance equation can be written in terms of the particle radius. Furthermore, the domain is divided into intervals of equal size ranges, which gives better numerical stability, but usually requires a very large number of intervals. Therefore, in order to obtain a solution without losing much information and taxing computer time, the domain is divided into a geometric series of particle sizes. In this work, similar to ^[13], a discretization factor of two is used, which means that each particle size interval is twice the size of the previous one, and each interval is represented by a characteristic volume that is the average of the upper and the lower boundary volumes of the interval. ^[13] By employing this method, the number of intervals is reduced considerably without losing valuable information. Consequently, in order to make Eq. [8] more amenable to numerical solution, the continuous population balance in Eq. [8] is replaced by the set of discretized equations represented by Eq. [9].

$$\frac{dN_k}{dt} = \sum_{i=1}^{i=k-2} 2^{i-k+1} N_{k-1} N_i W(r_{k-1}, r_i) + \frac{1}{2} N_{k-1}^2 W(r_{k-1}, r_{k-1}) - \sum_{i=1}^{k-1} 2^{i-k} N_i N_k W(r_i, r_k) - \sum_{i=k}^{\infty} N_i N_k W(r_i, r_k) - S_k N_k \quad [9]$$

The first two terms in Eq. [9] represent the generation of mass, the third and fourth terms represent the loss of mass both due to particle aggregation, and the term S_k accounts for particle removal from the melt by flotation. Determination of the particle collision rate, $W(r_i, r_k)$, and the particle flotation rate, S_k , has been described by Maniruzzaman and Makhlouf^[13].

III. VERIFICATION OF THE MODEL RESULTS

A. The Hydrogen Removal Model

In order to verify the predictions of the Hydrogen Removal model, molten commercial purity aluminum was held at 700°C in a silicon carbide crucible in an electrical furnace. Table I shows the pertinent experiment variables, the impeller rotation speed in this case was 450 rpm and the purge gas flow rate was 5 L/min. Computational fluid dynamics simulation of this system gives a mean turbulence energy dissipation rate of 2.91 m²/s³ and an argon gas volume fraction of 0.023. The hydrogen content of the melt was measured at various times during the degassing process, which lasted for 20 minutes, using an AlScan™ unit.

Figure 4 shows the measured hydrogen concentration vs. degassing time, as well as the computer predicted hydrogen concentration vs. degassing time curve. Note the excellent

agreement between the model predicted and the measured hydrogen concentration profiles.

B. The Particle Dynamics Model

In order to verify the predictions of the Particle Dynamics model, aluminum oxide powder of known particle size distribution was added to molten aluminum that was held at 750°C in an electrical furnace. The furnace was 0.224 m in diameter and 0.45 m high, and the initial melt depth was 0.3 m. A laboratory size rotary degasser was used to purge high purity argon gas into the melt. The diameter of the degasser's rotor shaft was 24 mm and the diameter of the cylindrical impeller was 80 mm. The gas was purged at a rate of 2 L/min through 12, eight mm diameter side holes that were equally spaced around the circumference of the impeller. The impeller was placed so that its bottom was 5 cm above the bottom of the furnace and was operated at 560 rpm. Computational fluid dynamics simulation of this reactor gives a mean turbulence energy dissipation rate of $0.333 \text{ m}^2/\text{s}^3$ and an argon gas volume fraction of 0.0725.

Molten samples were taken from the holding furnace before purging with argon and after purging for 20 minutes. The solidified samples were prepared using standard metallographic procedures, and the aluminum oxide particle size distribution in each sample was determined using image analysis.

AnalySIS 2.11 software manufactured and marketed by Soft Imaging System GmbH, Hammer Str. 89, D-48153 Münster, Germany.

A minimum of fifty fields from each sample was examined at 350X magnification, and the particle count per unit area was converted to particle count per unit volume using

standard stereological estimation techniques ^[13]. Figure 5 shows the measured particle concentration vs. particle radius curve after 20 minutes of purging with argon, as well as the computer predicted particle concentration vs. particle radius curve. Figure 5 shows that there is good agreement between the model predicted and the measured particle concentration profiles.

IV. COMPUTER SIMULATIONS AND DISCUSSION

The models were used to evaluate the change in aluminum oxide particle size distribution and hydrogen content during treatment of molten aluminum in a rotary degasser. The simulated system parameters are shown in Table I.

Figure 6 shows the change in hydrogen concentration in the melt with time for the rotary degasser operating at 450-rpm and two different purge gas flow rates. The initial hydrogen concentration in the melt and the hydrogen concentration at the melt's surface were 0.3 mL/100g of aluminum. Figure 6 shows that hydrogen removal is more efficient when using the high purge gas flow rate. The higher hydrogen removal efficiency at the higher purge gas flow rate is due to the higher volume fraction of purge gas in the melt and the smaller average stable bubble radius, both of which increase the total surface area of purge gas bubbles that is available for hydrogen pickup. Similarly, Figure 7 shows the change in hydrogen concentration in the melt with time for the rotary degasser operating at 5L/min purge gas flow rate and two different impeller speeds. Again, the initial hydrogen concentration in the melt and at the melt's surface was 0.3 mL/100g of aluminum. Although both impeller speeds reduce the hydrogen concentration in the melt

to about 0.05mL/100g of aluminum, the impeller rotating at 600 rpm achieves this low hydrogen concentration in approximately 10 minutes while the impeller rotating at 450 rpm requires 20 minutes to reduce the hydrogen concentration to this level.

The evolution of the particle size distribution was simulated by solving the discretized population balance, Eq. [9]. The initial particle radius range, which spanned the range 0.05 μm to 120 μm , was discretized into 35 sections each representing a particle radius sub range. The discretized ordinary differential equations system was solved using the explicit Euler method. Two inputs are necessary for calculating the particle collision rate. These are the mean turbulence dissipation rate (ϵ) and the volume fraction of purged gas. Warke et al ^[9] used computational fluid dynamics and calculated these parameters for a rotary degasser operating with the parameters shown in Table IV.

Table IV. Rotary Degasser Operation Parameters Used in the Simulations and Their Corresponding Mean Turbulence Dissipation Rate and Volume Fraction of Bubbles ^[9].

Case Number	Impeller Speed (rpm)	Gas Flow Rate (L/min)	Mean Turbulent Dissipation Rate (m^2/s^3)	Gas Volume Fraction
1	450	3	1.24	0.021
2	450	5	2.91	0.023
3	600	3	1.39	0.024
4	600	5	3.27	0.029

Other data necessary for calculating the particle collision rate and the rate of particle attachment to the rising gas bubbles is shown in Table V.

Table V. Physical Properties of Molten Aluminum and Aluminum Oxide ^[13].

Molten Aluminum at 973 K	
Density	2300 kg/m ³
Viscosity	0.0029 Pa-s
Surface tension	0.9 N/m
Kinematic Viscosity	1.3×10^{-6} m ² /s
Al ₂ O ₃ particles at 973 K	
Density	3500 kg/m ³
Hamaker Constant	0.45×10^{-20} J

Figure 8 shows the variation of the number of unwanted solid particles per cubic centimeter of molten aluminum with particle size for different purge gas flow rates. Larger particles are removed from the melt faster than smaller ones and the particle removal efficiency is higher at the high purge gas flow rate than at the low gas flow rate. This is due to the fact that the average stable bubble radius is smaller at the higher purge gas flow rate, and the fact that the volume fraction of gas in the melt increases with increasing gas flow rate. Figure 9 further illustrates the effect of gas flow rate on particle removal. Fig. 9 (a) shows the contribution of particles' attachment onto rising gas bubbles to the change in particle size distribution at two different purge gas flow rates, similarly, Fig. 9 (b) shows the contribution of Stokes flotation to the change in particle size distribution at two different purge gas flow rates.

Figure 10 shows the variation of the number of unwanted solid particles per cubic centimeter of molten aluminum with particle size for different rotation speeds. Particle removal is more effective at the higher impeller speed due essentially to the relatively high turbulence generated by the higher impeller speed, which increases the particles'

collision rate. Figure 11 further illustrates the effect of rotation speed on particle removal. Fig. 11 (a) shows the contribution of particles' attachment to rising gas bubbles to the change in particle size distribution at two different rotation speeds, similarly, Fig. 11 (b) shows the contribution of Stokes flotation to the change in particle size distribution at two different rotation speeds.

V. CONCLUSIONS

A model that describes the removal of dissolved hydrogen and the collision and removal of solid unwanted particles from molten aluminum alloys during rotary degassing is developed. The hydrogen removal module is based on a hydrogen concentration balance performed on the melt. The mass transfer coefficients at the melt/air interface and at the melt/bubble interface, as well as the equilibrium concentration of hydrogen at the melt/air interface are determined experimentally. The particle collision and removal module is based on the classical theory of turbulent agglomeration and is unique in that it accounts for both high and low intensity turbulent flow conditions. A particle population balance is used to describe the system mathematically, and a special discretization scheme is employed to reduce the computational complexity and the computer time required for solving the population balance equation. The model is verified by comparing its predictions to their experimentally obtained counterparts, and is used to investigate the effect of the rotary degasser's operational parameters on hydrogen removal and on the agglomeration of aluminum oxide particles and their removal from molten aluminum. The model is useful in the design and efficient operation of industrial rotary degassers.

NOTATIONS

A_s	Melt's free surface area	r_k	Radius of particle in the k -th interval
A_b	Total surface area of bubbles	S_k	Particle flotation rate
C^{eq}	Concentration of H at melt/air interface	S_v	Net rate of addition of new particles
C	Concentration of H in the melt	t	Time
C^b	Concentration of H at the center of bubble	V_{Al}	Volume of melt
K_b	Mass transfer coefficient at melt/gas bubble interface	v, \tilde{v}	Unit volume of fluid
K_s	Mass transfer coefficient at melt/air interface	W_e	Weber's number
I_v	Rate of change of volume of particle of volume v by transfer of material	W_v	Rate of collision between particles
N_k	Particle concentration in the k -th interval	W_s	Stokes collision rate
n_v	Particle size distribution density function	ρ	Density of melt
N_i	Total number of particles in the i -th interval	ε	Energy dissipation rate
Q_g	Gas flow rate	σ	Surface tension of the melt
r_b	Stable bubble radius		

REFERENCES

1. T. A. Engh: *Principles of Metal Refining*, Oxford University Press, New York, 1992, pp. 322-324.
2. M. Makhlouf, L. Wang, and D. Apelian: *Hydrogen in Aluminum Alloys-Its Measurement and its Removal*, a monograph published by AFS, Des Plaines, IL, 1998.
3. M. Maniruzamman and M. Makhlouf: *Phase Separation Technology in Aluminum Melt Treatment*", a monograph published by AFS, Des Plaines, IL, 2000.
4. O. Hjelle, T.A. Engh, and B. Rasch: *Int. Sem. Refining Alloying Liq. Alum. Ferro-alloys*, 1985, pp. 345-60.

5. B. Kulunk and R. Guthrie: *Light Met.*, 1992, pp. 963-975.
6. G. Sigworth: *Light Met.*, 2000, pp. 773-778.
7. E. M. Williams, R. W. McCarthy, S. A. Levy, and G. Sigworth, K.: *Light Met.*, 2000, pp. 785-793.
8. P. Bakke, J. Lauritzen, T.A. Engh, and D. Oymo: *Light Met.*, 1991, pp. 1015-23.
9. V. Warke, G. Tryggvason, and M. Makhoulf: Worcester Polytechnic Institute, Worcester, MA, 2003.
10. J. O. Hinze: *AIChE J.*, 1955, vol. 1, pp. 289-295.
11. S. T. Johansen, S. Gradahl, P. Tetlie, B. Rasch, and E. Myrobstad: *Light Met.*, 1998, pp. 805-810.
12. S. T. Johansen, R. Anvar, and B. Rasch: *Light Met.*, 1999, pp. 657-61.
13. M. Maniruzzaman, and M. Makhoulf: *Metall. Trans. B*, 2001, pp. 305-314.
14. H. H. Uhlig, and R. W. Revie: *Corrosion and Corrosion Control*, 3rd Edition, Wileys and Sons, 1985, pp. 190.
15. F. Gelbard and J. H. Seinfeld: *J. Comput. Phys.*, 1978, vol. 28, pp. 357-375.
16. J. D. Landgrebe and S. E. Pratsinis: *J. Colloid Interface Sci.*, 1990, vol. 139, pp. 63-86.
17. M. Frenklach and S. J. Harris: *J. Colloid Interface Sci.*, 1987, vol. 118, pp. 252-261.
18. J. J. Wu and R. C. Flagan: *J. Colloid Interface Sci.*, 1988, vol. 123, pp. 339-352.
19. M. J. Hounslow, R. L. Ryall, and V. R. Marshall: *AIChE J.*, 1988, vol. 34, pp. 1821-1838.

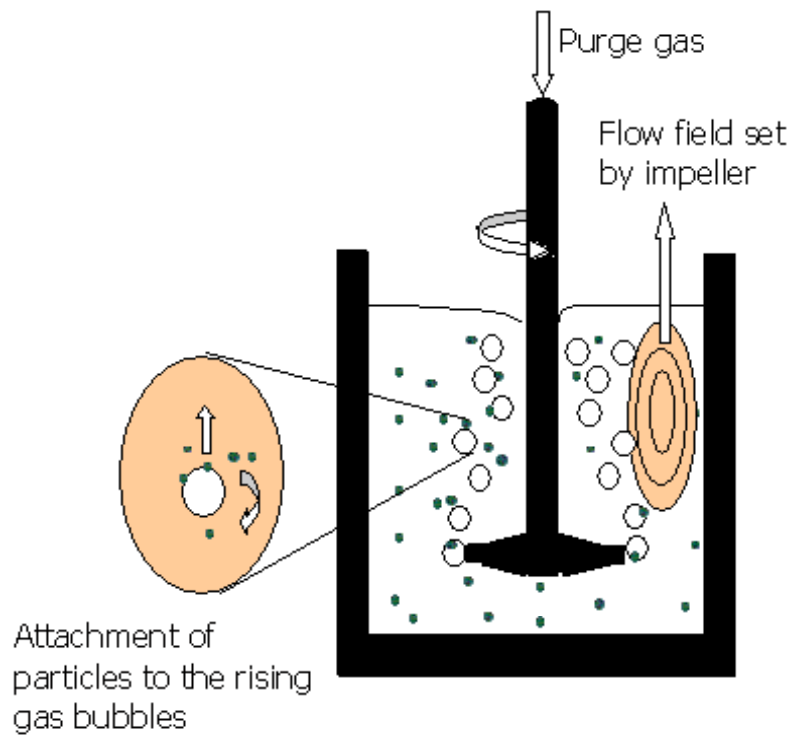


Fig. 1 – Schematic representation of the rotary degassing process.

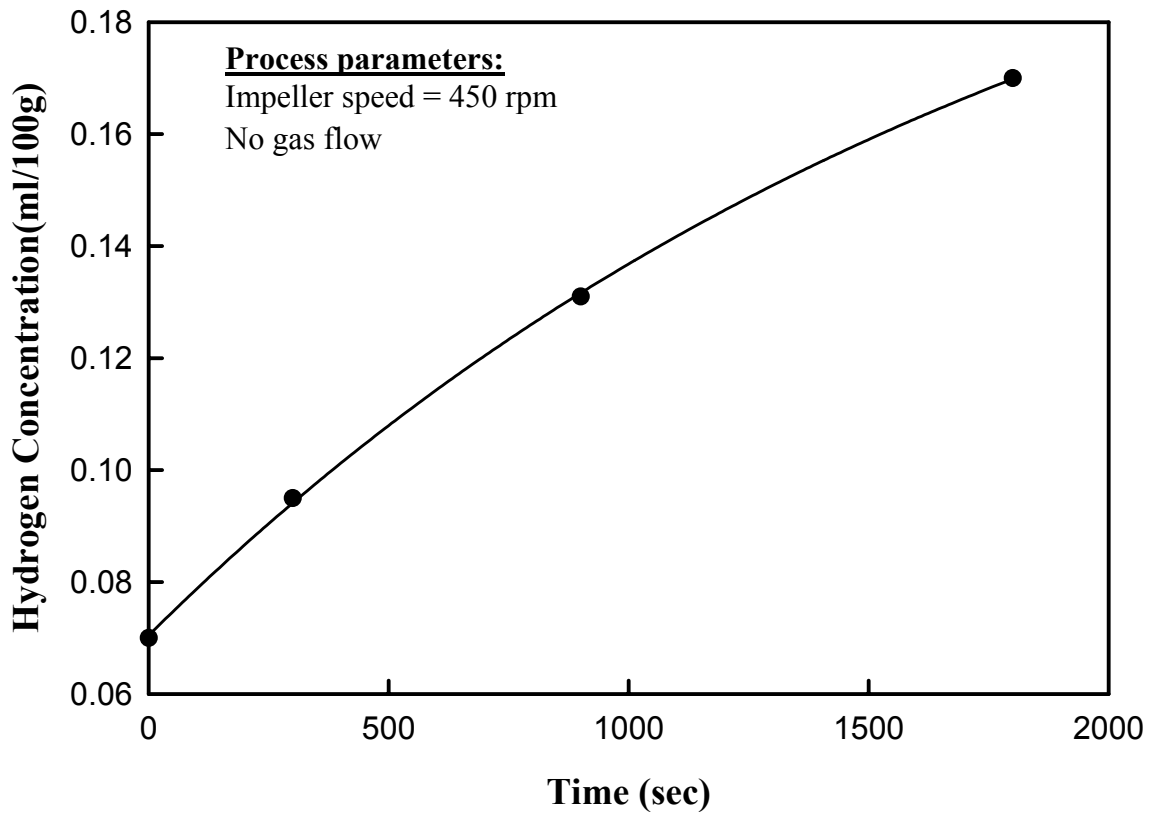


Fig. 2 – Variation of hydrogen concentration with time during melt stirring without the flow of purge gas.

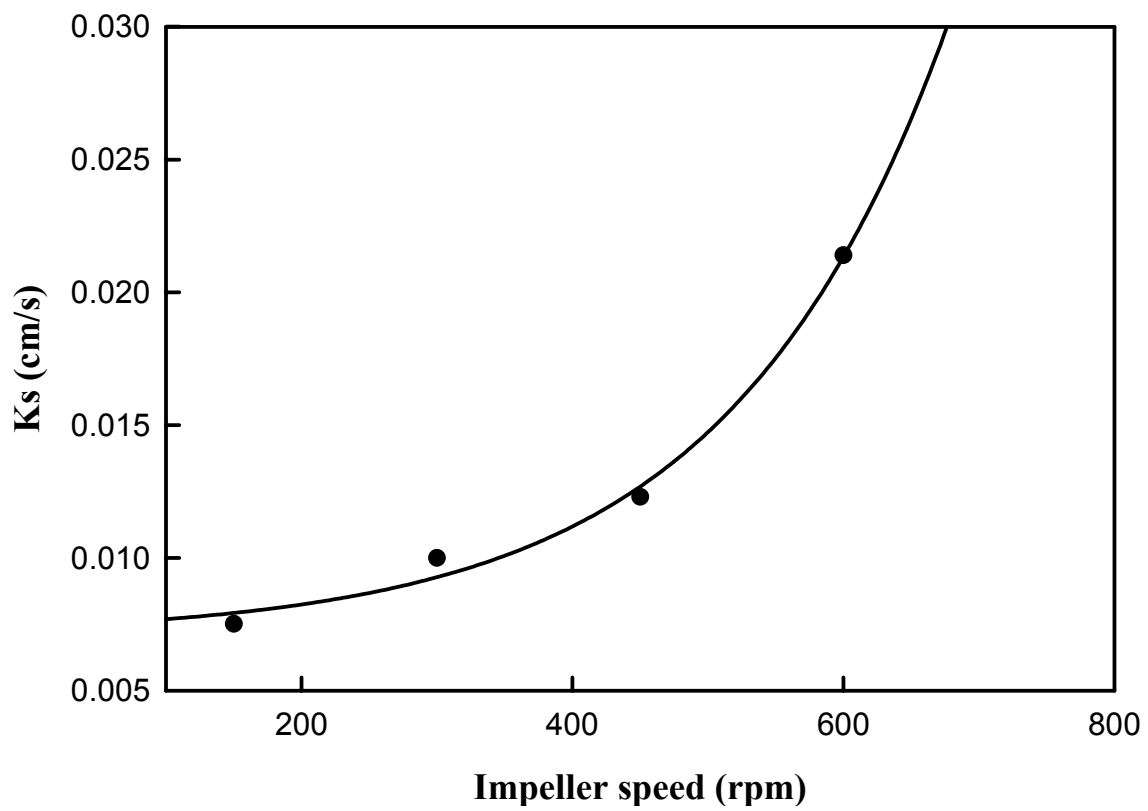


Fig. 3 – Variation of K_s with impeller speed.

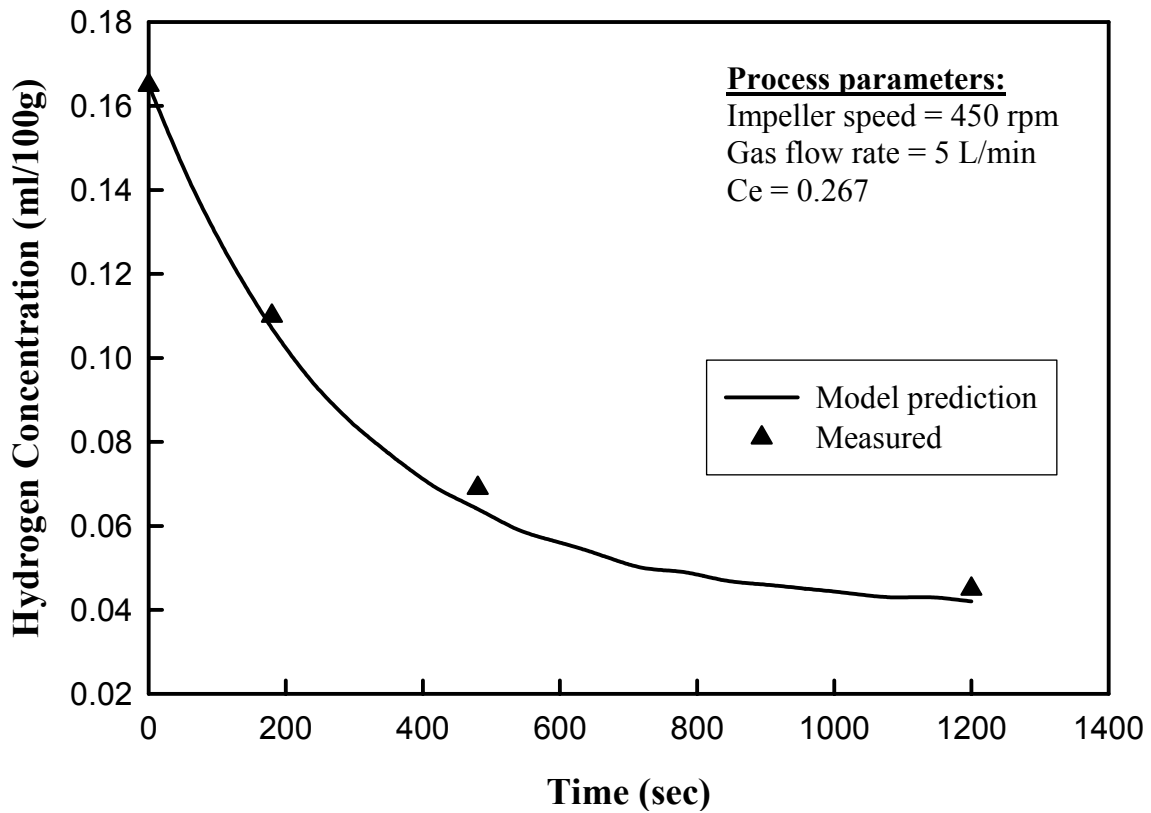


Fig. 4 – Verification of the hydrogen removal model prediction.

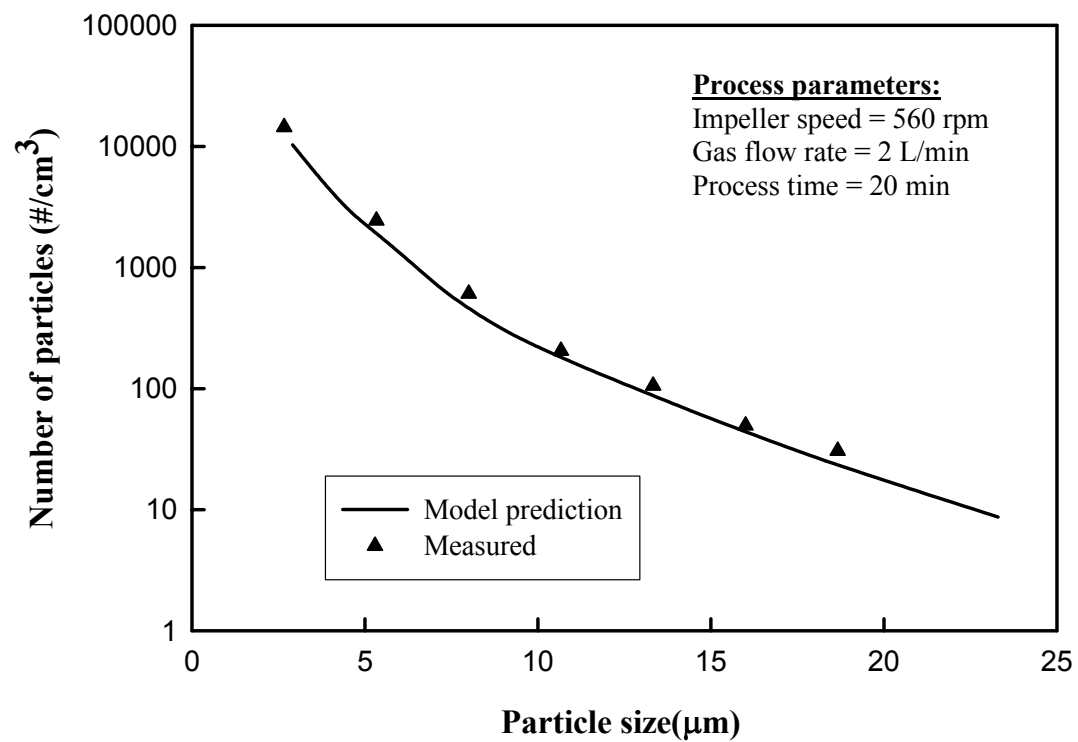


Fig. 5 – Verification of the particle dynamics model prediction.

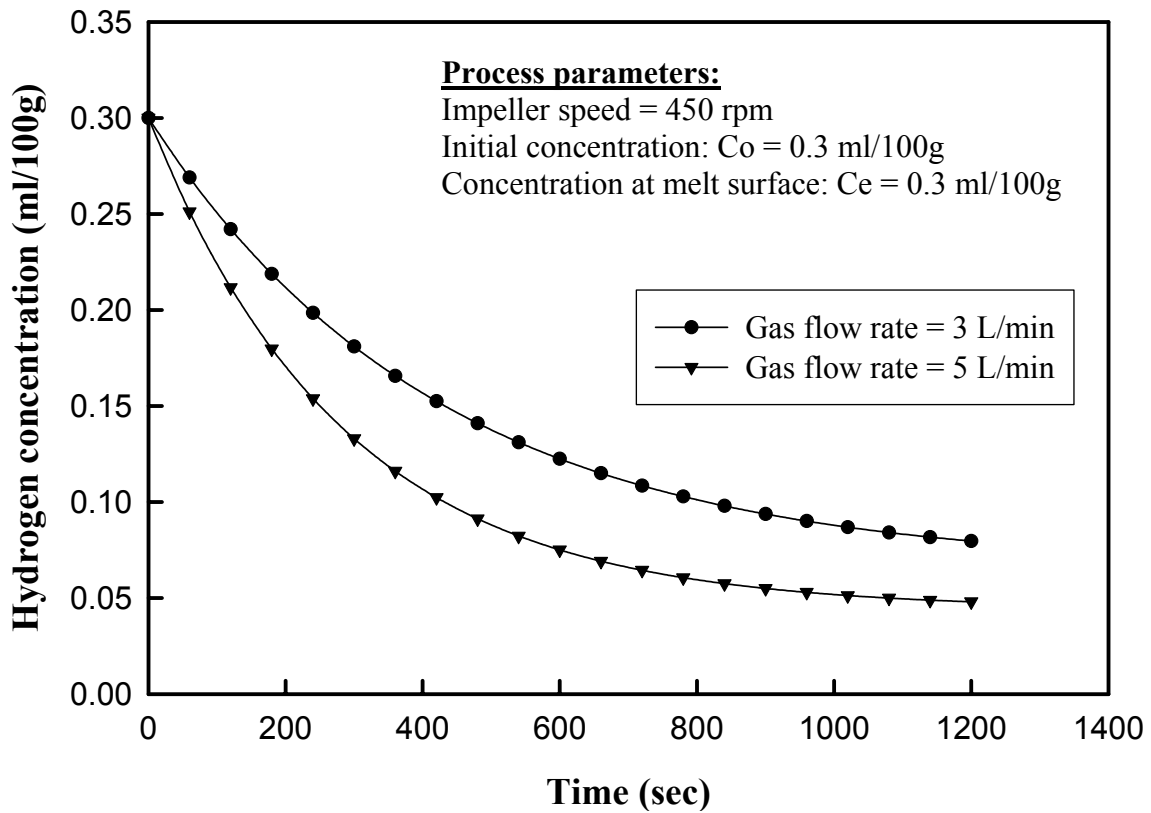


Fig. 6 – Model predicted variation of hydrogen concentration with time for different gas flow rates.

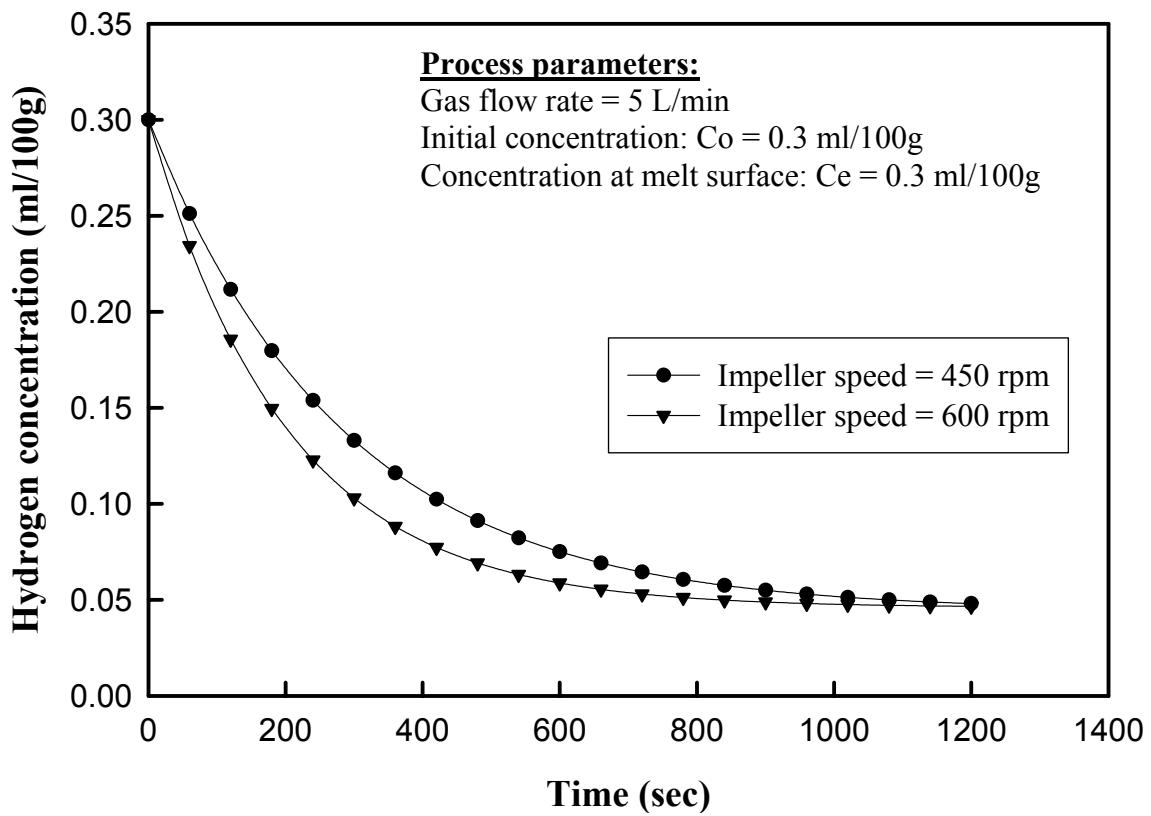


Fig. 7 – Model predicted variation of hydrogen concentration with time for different impeller speeds.

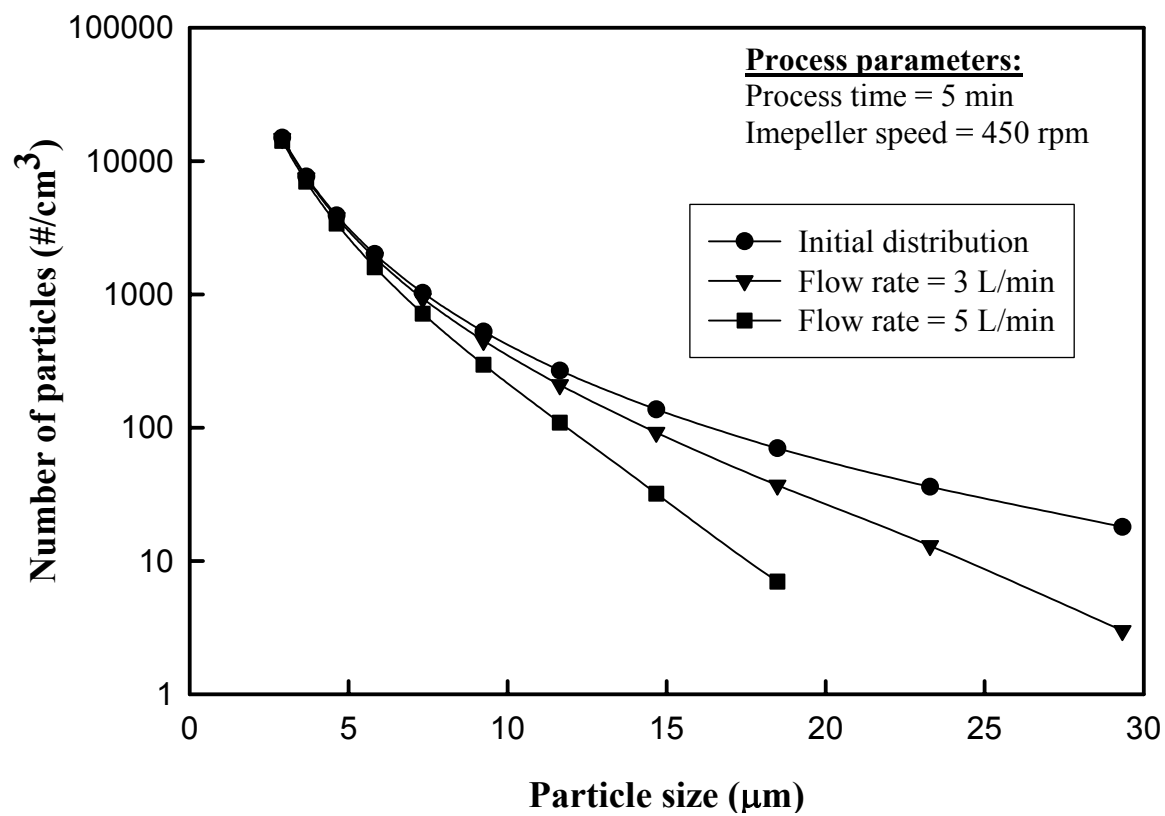


Fig. 8 – Model predicted variation of particle size distribution for different gas flow rates.

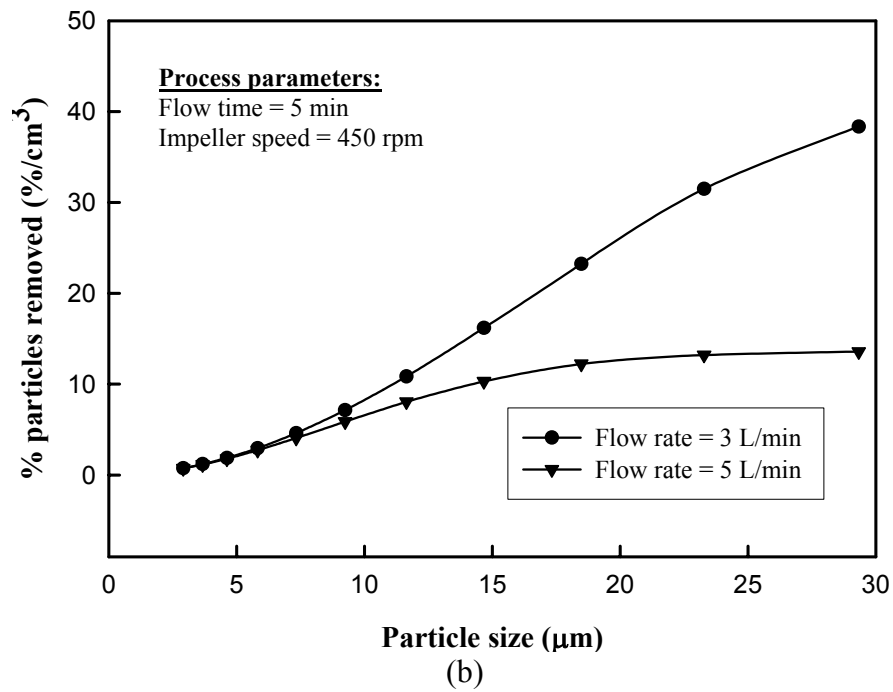
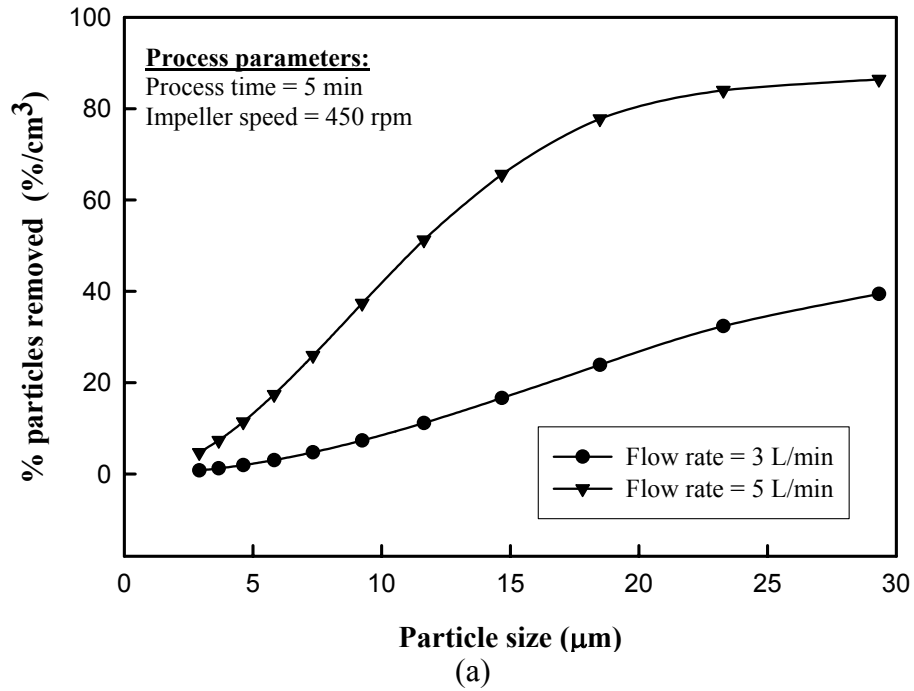


Fig. 9 – Model predicted variation of (a) % particles removed by bubble attachment, and (b) % particles removed by Stokes flotation, with particle size for different gas flow rates.

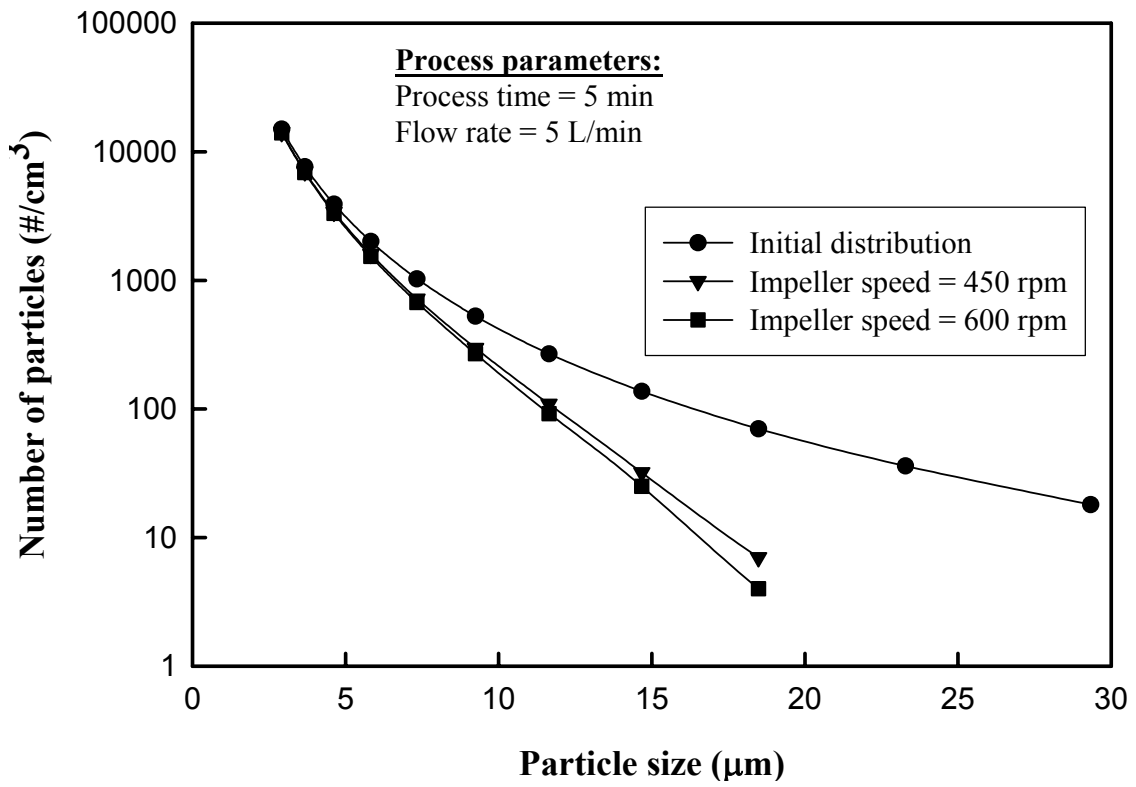
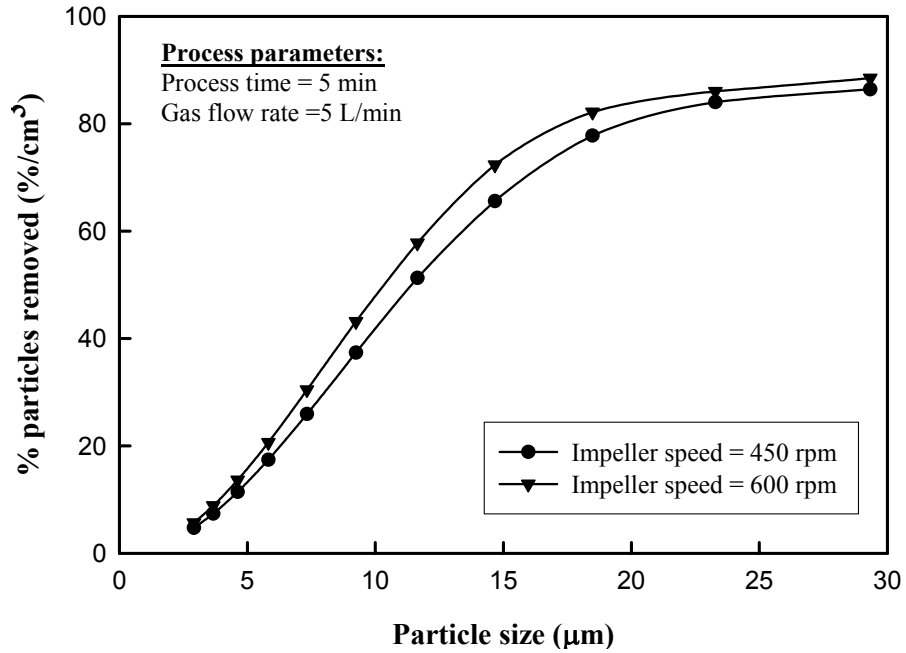
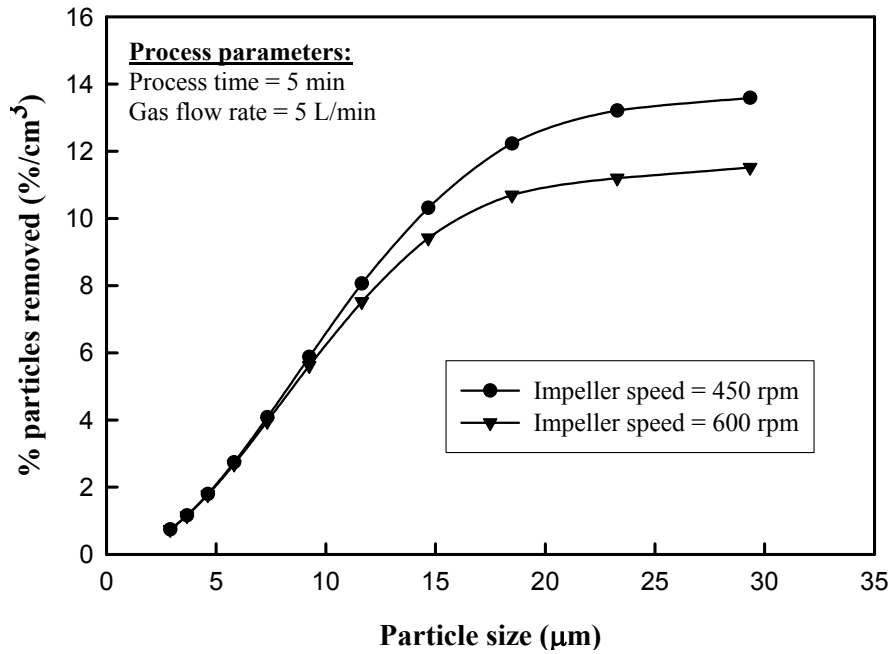


Fig. 10 – Model predicted variation of particle size distribution for different impeller speeds.



(a)



(b)

Fig. 11 – Model predicted variation of (a) % particles removed by bubble attachment, and (b) % particles removed by Stokes flotation, with particle size for different impeller speeds.

APPENDIX: A

The CFD Simulation

Purpose

This Appendix explains the step-by-step setup for running the CFD simulation of the rotary degasser using Fluent 6.0.2 solver. However the mesh generation is explicitly done in Gambit 2.0 and is not presented here.

Prerequisites

This article assumes that user is familiar with the Unix based operating system and preliminary commands necessary to open Fluent interface. In order to get started, first it is necessary to copy the mesh (case) file to the current working directory of the computer where all the simulation data is going to be generated. Copy the file named themodel.cas from the CD. This file contains the mesh information as well as the preset boundary conditions to run the problem under steady state.

Setup and Solution

Most of the parameters are already preset in the given case file, however the checklist is as follows for the reference.

Note: Words in bold and italic format shows the menus and buttons in Fluent graphical user interface.

Step 1: Grid

1. Read the file themodel.cas in the 3-D version of Fluent.

Directions: *File > Read > Case....*

2. Check the grid to make sure no mesh volume or area appears negative.

Directions: **Grid > Check**

3. Display the grid using following steps:
 - **Grid > Display**; This will open the grid display panel.
 - Under **Options** select **Edges** and set **Edge type** to **All**.
 - Under **Surfaces** select everything except **default-interior**, **default-interior:001**, **wall-17**, and **wall-18** and click **Display**. It will show the grid in new window.
 - In order to rotate the view, go to **Display > Views** and click on the **Camera**, it will open the **camera parameter** window. Turn the dial showing arrow until the image rotates through 90°.

Step 2: Grid Interfaces

Since the mesh is nonconformal, the grid interfaces are needed to be setup. The given case file contains the grid interfaces already setup; however the checklist to this setup is as follows

1. **Define > Grid Interface**; will open **Grid interfaces** panel.
2. Under **Grid Interface** menu, enter name as “int”
3. Under **Interface Zone 1**, select **interface-1** and under **Interface Zone 2**, select **interface-2** and click **Create**.
4. **Close** the Grid Interfaces panel.

Step 3: Models

1. **Define > Model > Solver**; Select **Segregated** and **Steady** in the **Solver** panel.

2. **Define > Model > Multiphase**; Select **Eulerian** in the **Multiphase model** panel.
3. **Define > Model > Viscous**; Select **k-epsilon Model** in the **Viscous model** panel and accept the default parameters.

Step 4: Materials

1. **Define > Material**; type in the name of fluid as Al- melt, Under Properties section input density as 2300 Kg/m³, and viscosity as 0.0029 Pa-s. Click on Create. Copy Argon from the database and retain its properties.
2. **Define > Phases**; set the primary phase as Al-melt and secondary phase as argon.

Step 5: Operating Conditions

1. **Define > Operating Conditions**; turn on **gravity**, Under **Gravitational Acceleration**, the value of **X** should be **-9.81**.

Step 6: Boundary Conditions

The boundary conditions are already preset in given case file. However check each setting with respect to following list.

1. **Define > Boundary Conditions**; will open the boundary condition panel.
2. Under **Zone**, select **cylinder**, set the **Type** to **wall**.
3. For **top**, select **pressure outlet**, and set **Backflow Volume Fraction** for **argon** as **1**.
4. For **disk**, set the **Type** to **wall** and click on the **Set**
 - **Wall Motion: Moving wall**
 - **Motion: Relative to adjacent cell zone and Rotational**
 - **Speed: 0 rpm**

- *Rotation axis direction (X, Y, Z) as (1,0,0)*
5. For *shaft*, set the *Type* to *wall* and click on the *Set*
 - *Wall Motion: Moving wall*
 - *Motion: Relative to adjacent cell zone and Rotational*
 - *Speed: 450 rpm*
 - *Rotation axis direction (X, Y, Z) as (1,0,0)*
 6. For *inlet 1* through *4*, set the *Type* to *wall* and click on the *Set*
 - *Wall Motion: Moving wall*
 - *Motion: Relative to adjacent cell zone and Rotational*
 - *Speed: 0 rpm*
 - *Rotation axis direction (X, Y, Z) as (1,0,0)*
 7. For *diskfluid*, set the *Type* to *fluid* and click on the *Set*
 - *Rotation axis direction (X, Y, Z) as (1,0,0)*
 - *Motion Type: Moving Reference Frame*
 - *Speed (rpm): 450 rpm*
 8. For *tankfluid*, set the *Type* to *fluid* and click on the *Set*
 - *Rotation axis direction (X, Y, Z) as (1,0,0)*
 - *Motion Type: Stationary fluid.*

Step: 7 Solution

The problem is solved in two stages. The initial part of the solution is obtained for a single-phase flow field with steady flow. The later part of the solution is obtained for unsteady flow, using MRF and solving volume fraction equation.

Solution 1: Solve for single-phase flow field in steady state.

1. *Solve > Initialize > Initialize..* ; will open *Solution Initialization* panel , click on *init*.
2. *Solve > Controls > Solutions*; will open *Solution Controls* panel. Deselect the *volume fraction* under *Equations* and click *ok*.
3. *Solve > Monitors > Residuals*; make sure both *print* and *plot* options are selected.
4. *Solve > Iterate*; Under *Number of Iterations* input 1500, and click on *Iterate*.

Note: The number of iterations required for convergence may be different for different machine configuration.

Solution 2: Solve for multiphase unsteady problem.

Note: The unsteady solution must be started only after the converged steady state solution.

1. Under *Boundary Conditions*, set all *inlet 1* through *4* set Type to *Velocity Inlet*, it will open the question dialog, click on the *Yes* button.
2. Under *phase* in *Boundary Condition* panel select *argon*. Click on the *Set..* button for each inlet i.e. *inlet 1* through *4* .
 - *Velocity Specification Method: Component*
 - *Reference Frame: Absolute*
 - *Co-ordinate System: Cylindrical*
 - *Radial-velocity: 23 m/s*
 - *Tangential-velocity: 0 m/s*
 - *Axial-velocity: 0 m/s*
 - *Angular-velocity: 0 rpm*

- *Volume fraction: 1*
3. Set the *Define > Model > Solver* to *unsteady* in the *Solver* panel.
 4. In the *Solution Controls* panel, set the *Under-Relaxation Factors* for *Momentum* as *0.4*, for *Pressure* as *0.3*, for *Volume Fraction* as *0.2*, for the rest retain default values. Select the *Volume Fraction* under *Equations*.
 5. Before starting iterations, set commands to auto save case and data files in order to post process the data.
 - *File > Write > Autosave* ; will open *Autosave case/data* panel, put *100* each for *Autosave case file* and *Autosave data file frequency* and set the path under *Filename* pointing to the directory where these file will be saved, for example “/research/viren/TheModel/450rpm-3Lpermin.gz” , Fluent solver will automatically save the case and data file after 100 time steps in compressed tar.gz file format.
 - *Solve> Monitors > Volumes*; will open the Volume monitors panel. Change the *volume monitor* number to *1*. Under *name* type *vfargon* , select *plot* and *write*. Under *Every* select *Time Step* and click on *Define*. It will open *Define Volume Monitor* panel. Under *Report Type* select *Volume-average*. Under *X axis* select *Flow Time*, Select *Field variables* as *phases* and *volume fraction of argon*. Under cell zone select both cell zones in the list and set the directory path under *File Name*. This setting will plot and write the volume fraction of argon gas with flow time as shown in fig.1

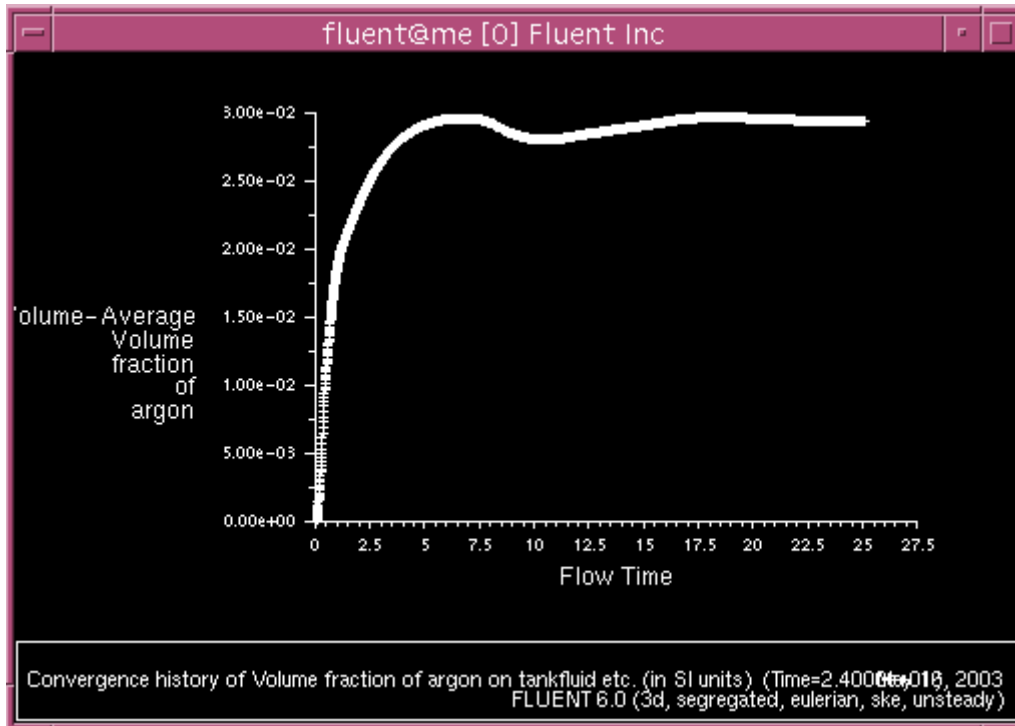


Fig.1- Variation of Volume fraction of argon with Flow time.

6. In the *Iterate* panel set the *Time Step Size* to *0.01* s, and *Number of Time Steps* to *2400*. This will cover the flow time of 24 seconds.

Step 8: Data post processing

1. Plotting contours and velocity vectors on specific plane of 3-D geometry
 - To create a virtual plane, go to *Surfaces > Iso-surface*, Select *Grid* and *Y-coordinate* under *Surface of Constant* and click *create*
 - Create another Iso-surface with *X-coordinate* and *Iso-value* as 3.
2. *Display > Contours*; will open the *Contours panel*, Select *Filled*, *Node value*, *Global range*, *Auto range* under *Options*. Select *Contour of Phases* and *Volume fraction of argon*. Under *Surfaces* select *Y-coordinate-14* and click *Display*. Fig 2 shows the contours of volume fraction of argon gas after 24 sec.

3. **File > Hardcopy**; will open the **Graphics hardcopy** panel, Select the format in which image to be saved and Click on **Save**.

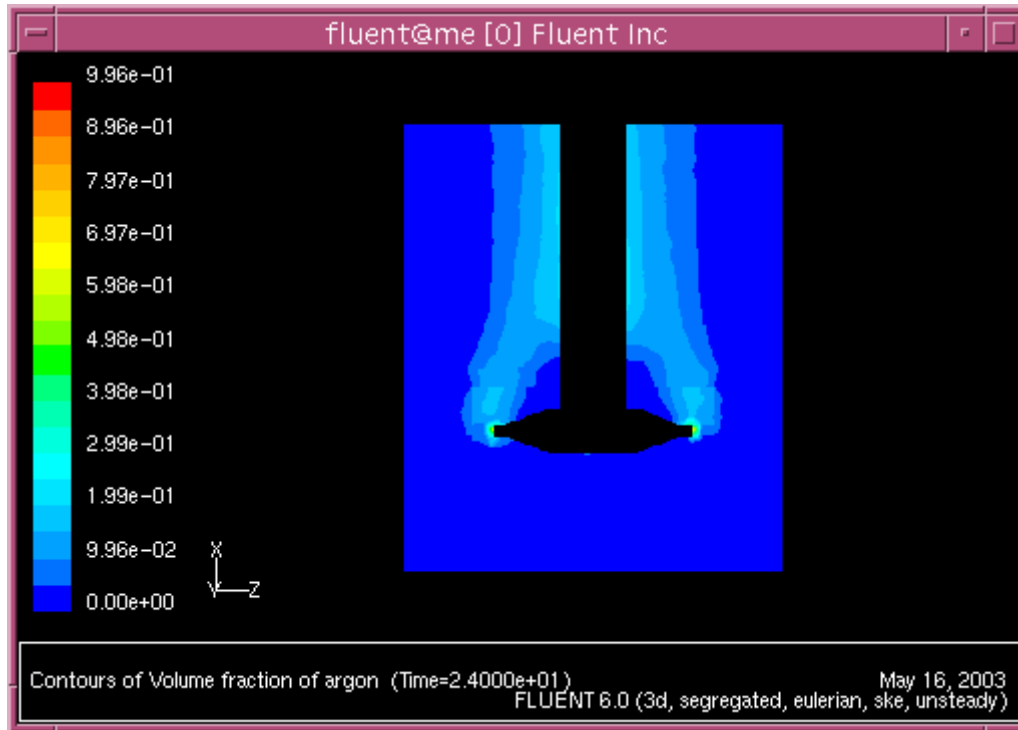


Fig. 2- Contours of Volume fraction of Argon gas after 24 sec.

4. In order to compute the volume averaged, volume fraction of argon and energy dissipation rate, go to **Report > Volume Integrals**, Under **Options** select **Volume-Average**, Select **Phases** and **Volume fraction of argon** under **Filed Variable** and select both **Cell Zones**. Click on **Compute** will give the result under **Volume-weighted Average field**. Same procedure can be employed to compute volume-weighted average of energy dissipation rate.

APPENDIX: B

The Particle Dynamics Simulation

Purpose

This Appendix explains the step-by-step setup for running the particle dynamics simulation. This simulation is written in Visual Basic and interfaces with the C++ program that runs in background.

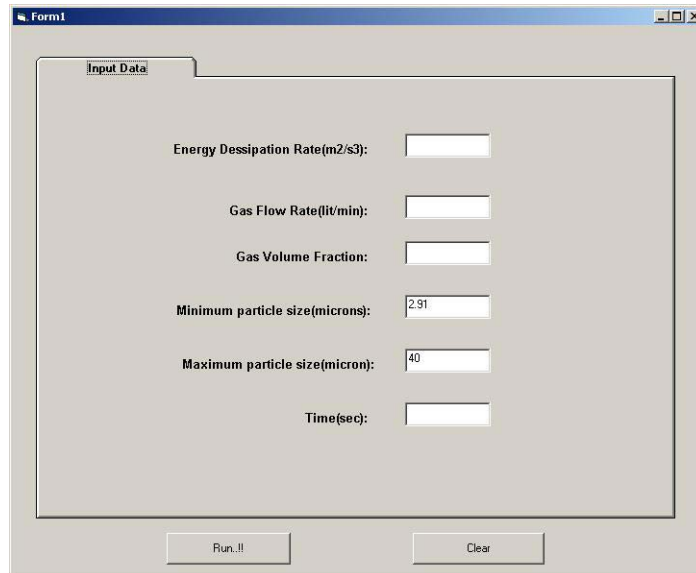
Prerequisites

In order to get started, first it is necessary to run setup from the package given in the CD. Run setup.exe file from this folder, it will install the software on the local hard drive. (This requires to be done only once). This module runs only on windows based machines.

Note: This module requires input data, to be obtained from the CFD simulations explicitly.

Setup and Solution:

1. In windows environment go to *Start > Program > Particle Dynamics Model*, this will open the graphical user interface as shown in fig. 1



The screenshot shows a Windows-style window titled "Form1". Inside the window, there is a tab labeled "Input Data". Below the tab, there are six input fields, each with a label and a text box:

- Energy Dissipation Rate(m2/s3): []
- Gas Flow Rate(lit/min): []
- Gas Volume Fraction: []
- Minimum particle size(microns): [2.91]
- Maximum particle size(micron): [40]
- Time(sec): []

At the bottom of the window, there are two buttons: "Run!!" and "Clear".

Fig.1- Main Screen

2. Input all the required data in the *input data* panel, as shown in fig. 1 and Click on **Run**, a question dialog will appear, click OK to start C++ program interface. The C++ code will run in the background and another question dialog will appear when C++ code is done and all other panels will be visible as shown in fig.2

The screenshot shows a window titled "Form1" with four tabs: "Input Data", "OutputTable", "Distribution Plot", and "Removal Plot". The "Input Data" tab is active and contains the following fields and values:

Parameter	Value
Energy Dissipation Rate(m2/s3):	3.27
Gas Flow Rate(lit/min):	5
Gas Volume Fraction:	0.029
Minimum particle size(microns):	2.91
Maximum particle size(micron):	40
Time(sec):	600

At the bottom of the "Input Data" panel, there are two buttons: "Run !!" and "Clear".

Fig. 2- Screen after C++ code is complete

3. The *Output Table* panel shows the list of particles size distribution initially and after the specified time. It also tabulates the % particle removal statistics. Fig 3 shows the *Output Table* panel.

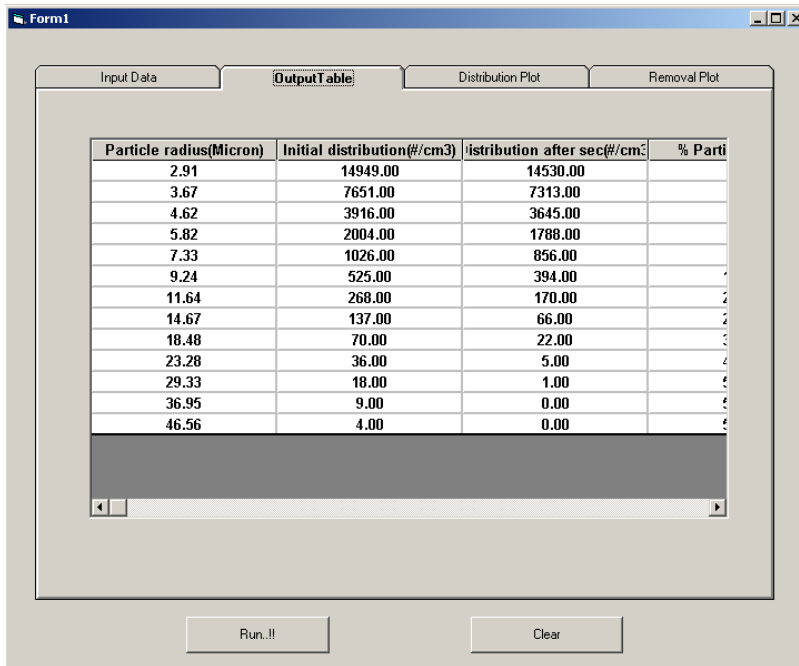


Fig. 3-Output Table showing the particle statistics before and after degassing.

- The **Distribution Plot** panel shows the particle size distribution curve before and after degassing. Two buttons on the bottom right toggles the Y-axis scale of the plot between linear and Log scales as shown in Fig. 4

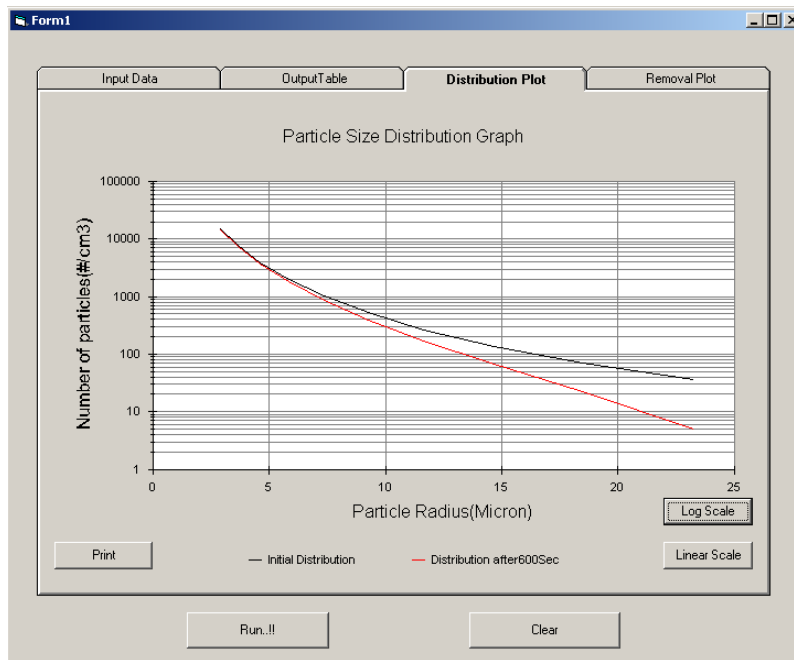


Fig. 4- Distribution Plots

5. The **Removal Plot** panel shows curves for the % particles removed by flotation and sinking. Fig. 5 shows the removal plot panel.

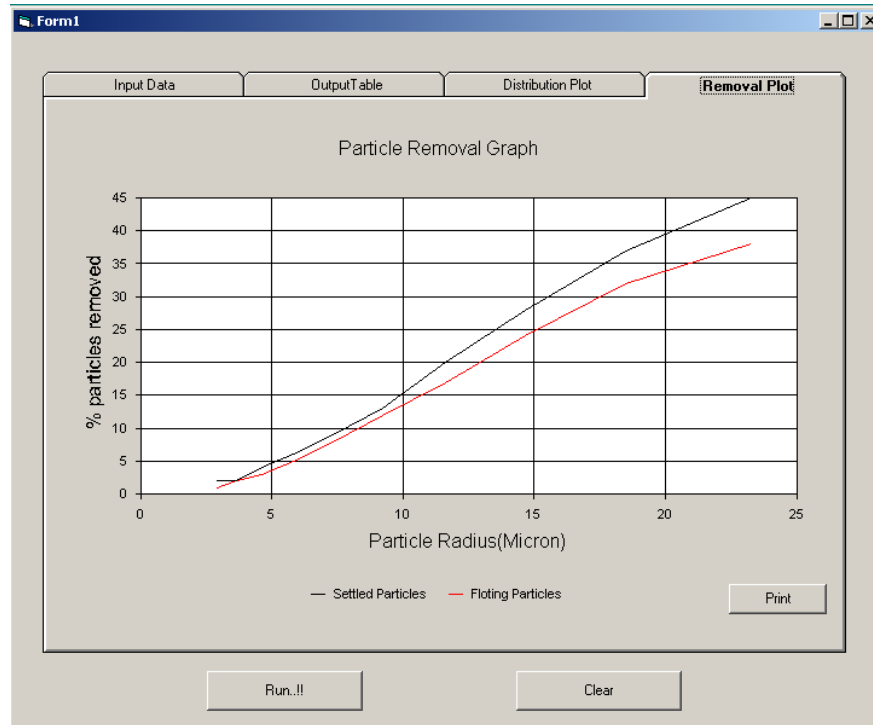


Fig. 5- Removal plots.

6. This module also writes text files on the hard drive (C:) , with file name all_rates.txt .This file can be imported into external plotting software such as Microsoft Excel or Sigma Plot to get better quality graphs.

APPENDIX: C

The Hydrogen Removal Simulation

Purpose

This Appendix explains the step-by-step setup for running the Hydrogen removal simulation. This simulation is written in C++ program that runs under dos console.

Prerequisites

In order to get started, first it is necessary to copy file named Hydrogen.exe from CD to the current working directory on the windows machine.

Note: This module requires input data, to be obtained from the CFD simulations explicitly.

Setup and Solution

1. Double click on the Hydrogen.exe; the program will open in console-based window.
2. The program will ask user a series of questions as follows.
 - Enter the initial concentration of Hydrogen (ml/100g):
 - Enter the concentration of Hydrogen at surface (ml/100g):
 - Enter total surface area of bubbles (cm²):
 - Enter process time (sec):
3. The program will close automatically after entering the time.
4. The output file will be generated with the name H-Predicted.txt that can be imported into external plotting software such as Microsoft Excel or Sigma Plot to generate the Hydrogen Concentration profile with time graphs.